






Predicting dark respiration rates of wheat leaves from hyperspectral reflectance

Onoriode Coast¹  | Shahen Shah^{1,2} | Alexander Ivakov³ | Oorbessy Gaju¹ | Philippa B. Wilson¹  | Bradley C. Posch¹ | Callum J. Bryant¹ | Anna Clarissa A. Negrini¹ | John R. Evans³  | Anthony G. Condon^{3,4} | Viridiana Silva-Pérez^{3,4} | Matthew P. Reynolds⁵ | Barry J. Pogson¹ | A. Harvey Millar⁶  | Robert T. Furbank^{3,4} | Owen K. Atkin¹ 

¹ARC Centre of Excellence in Plant Energy Biology, Research School of Biology, Australian National University, Canberra, Australian Capital Territory 2601, Australia

²The University of Agriculture Peshawar, Peshawar 25130, Pakistan

³ARC Centre of Excellence for Translational Photosynthesis, Research School of Biology, Australian National University, Canberra, Australian Capital Territory 2601, Australia

⁴CSIRO Agriculture, Canberra, Australian Capital Territory 2601, Australia

⁵International Maize and Wheat Improvement Centre (CIMMYT), México 06600, Mexico

⁶ARC Centre of Excellence in Plant Energy Biology, University of Western Australia, Perth, Western Australia 6009, Australia

Correspondence

Owen K. Atkin, ARC Centre of Excellence in Plant Energy Biology, Research School of Biology, Australian National University, Canberra, ACT 2601, Australia.
Email: owen.atkin@anu.edu.au

Present Address

Alexander Ivakov, Australian Institute of Sport, Leverrier Street, Bruce, ACT, 2617 Australia;

Philippa B. Wilson, Grains Research and Development Corporation, Kingston, ACT 2604, Australia.

Funding information

Australian Government Endeavour Fellowship; International Wheat Yield Partnership, and Grains Research Development Council, Grant/Award Number: ANU00027; Australian Government National Collaborative Research Infrastructure Strategy (Australian Plant Phenomics Facility); Centre of Excellence for Translational Photosynthesis, Australian Research Council, Grant/Award Number: CE1401000015; Centre of Excellence in Plant Energy Biology, Australian Research Council, Grant/Award Number: CE140100008

Abstract

Greater availability of leaf dark respiration (R_{dark}) data could facilitate breeding efforts to raise crop yield and improve global carbon cycle modelling. However, the availability of R_{dark} data is limited because it is cumbersome, time consuming, or destructive to measure. We report a non-destructive and high-throughput method of estimating R_{dark} from leaf hyperspectral reflectance data that was derived from leaf R_{dark} measured by a destructive high-throughput oxygen consumption technique. We generated a large dataset of leaf R_{dark} for wheat (1380 samples) from 90 genotypes, multiple growth stages, and growth conditions to generate models for R_{dark} . Leaf R_{dark} (per unit leaf area, fresh mass, dry mass or nitrogen, N) varied 7- to 15-fold among individual plants, whereas traits known to scale with R_{dark} , leaf N, and leaf mass per area (LMA) only varied twofold to fivefold. Our models predicted leaf R_{dark} , N, and LMA with r^2 values of 0.50–0.63, 0.91, and 0.75, respectively, and relative bias of 17–18% for R_{dark} and 7–12% for N and LMA. Our results suggest that hyperspectral model prediction of wheat leaf R_{dark} is largely independent of leaf N and LMA. Potential drivers of hyperspectral signatures of R_{dark} are discussed.

KEYWORDS

high-throughput phenotyping, leaf reflectance, machine learning, mitochondrial respiration, proximal remote sensing, wheat (*Triticum aestivum* L.)

1 | INTRODUCTION

The world's population is projected to rise by approximately 30%, reaching 9.7 billion in 2050 (United Nations Department of Economic and Social Affairs Population Division, 2015). This increase will cause demand for staple food crops to double (Cassman, 1999; Tilman, Balzer, Hill, & Befort, 2011). Doubling crop productivity to match future demand will be challenging (Tilman, Cassman, Matson, Naylor, & Polasky, 2002), a challenge exacerbated by climate change (Goldsmith, Gunjal, & Ndarishikanye, 2004; Intergovernmental Panel on Climate Change, 2013; Xiao & Ximing, 2011). Addressing these challenges will require the simultaneous pursuit of a broad range of options (Godfray et al., 2010) including increasing yield per unit of land, and identification and use of germplasm with better resilience to global climate change.

Theoretically, increasing radiation use efficiency (RUE, increase in biomass per unit absorbed radiation) provides a novel way to increase potential yield. RUE could be increased by improving photosynthesis by (a) altering crop canopy architecture to alter the distribution of radiation capture between leaves (Loomis & Williams, 1969); (b) introducing a carbon concentrating C_4 mechanism into C_3 plants (Furbank, von Caemmerer, Sheehy, & Edwards, 2009); and (c) re-engineering Rubisco (Parry, Madgwick, Carvalho, & Andralojc, 2007). Another opportunity to increase RUE is to optimize mitochondrial respiration in the dark (R_{dark}). In all plants, energy from R_{dark} drives biosynthesis, cellular maintenance, and active transport. The respiratory pathway also provides intermediates that serves as substrates for the synthesis of adenosine triphosphate (ATP), amino acids, nucleic acids, fatty acids, and many secondary metabolites. The efficiency of ATP synthesis per unit of CO_2 released or O_2 consumed through the respiratory process varies, depending on engagement of phosphorylating and nonphosphorylating pathways of mitochondrial electron transport (Millar, Whelan, Soole, & Day, 2011; Vanlerberghe & McIntosh, 1997). Variations in the rate and efficiency of leaf R_{dark} thus have the potential to influence biomass accumulation and yields of crops (Hauben et al., 2009; Wilson & Jones, 1982). Consequently, large datasets on leaf R_{dark} have potential application in various aspects of the crop production system, including screening of germplasm in genetic resource collections and in plant breeding; assessing the efficacy of agricultural management programmes; and monitoring crop health. Of particular importance is the formation of comprehensive datasets that assess genotype- and environment-mediated variation in leaf R_{dark} under controlled and field conditions.

Leaf respiration, defined as the nonphotorespiratory mitochondrial CO_2 evolution in the light (R_{light}), is typically less than R_{dark} (Hurry et al., 2005; Pärnik & Keerbergh, 1995). Techniques for measuring R_{light} , including the Laisk (1977), Kok (1948), and mass spectrometry (Loreto, Velikova, & Di Marco, 2001) approaches, are low throughput and often challenging to correctly implement. Measuring R_{dark} is also slow and cumbersome. To address the issue of low-throughput methods to measure leaf respiration, high-throughput approaches have been recently developed to estimate R_{dark} by measuring O_2 consumption

(O'Leary et al., 2017; Scafaro et al., 2017; Sew et al., 2013). Sew et al. (2013) employed a liquid-phase oxygen-sensitive fluorophore technology, whereas Scafaro et al. (2017) and O'Leary et al. (2017) used a faster, automated gas-phase method; the latter system takes only ~1–2 min per sample. Such high-throughput measurements of respiratory O_2 uptake will be indicative of rates of CO_2 efflux in leaves where the primary respiratory substrate is sucrose and the latter is fully oxidized to CO_2 and H_2O (Lambers, Chapin, & Pons, 2008). However, whereas these approaches enable rapid screening of large numbers of samples, all require destructive sampling of leaves, limiting their utility for ongoing monitoring of leaf R_{dark} at the landscape scale. In the current study, we outline a rapid non-destructive technique—using reflectance spectra—to estimate R_{dark} .

Instruments can measure electromagnetic radiation reflected from vegetation surfaces spanning the visible (400–700 nm), near-infrared (NIR, 700–1300 nm), and shortwave infrared (SWIR, 1400–3000 nm) spectral regions. When light falls on a leaf, it can be absorbed, reflected, or transmitted. Light absorption by leaves in the visible region is driven by electron transitions in pigments (including chlorophyll, carotenoids, and anthocyanins). In the NIR–SWIR spectral region of 700–2400 nm, in contrast, light absorption is driven by the bending and stretching of covalent bonds between hydrogen atoms and atoms of carbon, oxygen, and nitrogen in water and other chemicals (Curran, 1989). Radiation reflected from leaves can provide information about the internal composition of the leaf (Blackburn, 2007; Jacquemoud et al., 1996; Jacquemoud & Baret, 1990). Reflectance over a broad range of narrow and contiguous wavelength bands, termed hyperspectral reflectance, is increasingly used to predict plant or crop traits including water status (Gutierrez, Reynolds, & Klatt, 2010; Sims & Gamon, 2003); photosynthetic metabolism (Ainsworth, Serbin, Skoneczka, & Townsend, 2014; Barnes et al., 2017; Serbin, Dillaway, Kruger, & Townsend, 2012; Silva-Pérez et al., 2018); leaf mass per area (LMA; (Asner et al., 2011; Asner & Martin, 2008; Ecartot, Compan, & Roumet, 2013); concentrations or contents of nitrogen (N), lignin, and photosynthetic pigments (Martin & Aber, 1997; Yendrek et al., 2017); and grain yield (Montesinos-López, Montesinos-López, Crossa, et al., 2017; Montesinos-López, Montesinos-López, Cuevas, et al., 2017; Weber et al., 2012).

Respiration rates at a standard temperature (25°C , R_{dark}^{25}), whether expressed on a mass or area basis, are highly variable. Variation in R_{dark}^{25} among genotypes and environments is predictable from other leaf traits such as N concentration or content, LMA, and the carboxylation capacity of Rubisco at 25°C ($V_{\text{c,max}}^{25}$; Atkin et al., 2015; Reich, Walters, Ellsworth, et al., 1998; Reich, Walters, Tjoelker, Vanderklein, & Buschena, 1998; Ryan, 1991). Both N and LMA can be predicted from hyperspectral reflectance data (Ecartot et al., 2013; Serbin et al., 2012; Silva-Pérez et al., 2018). It is also possible to predict $V_{\text{c,max}}^{25}$, but with lower accuracy and precision (Ainsworth et al., 2014; Dechant, Cuntz, Vohland, Schulz, & Doktor, 2017; Doughty, Asner, & Martin, 2011; Serbin et al., 2012; Silva-Pérez et al., 2018). The poorer ability to predict $V_{\text{c,max}}^{25}$ from leaf reflectance compared with leaf N could be due to the absence of a direct absorption signal related to $V_{\text{c,max}}^{25}$, arising instead from a secondary

correlation with leaf N (Dechant et al., 2017). Both photosynthesis and respiration are processes requiring numerous proteins (Evans, 1989a; Evans & Terashima, 1988; Field & Mooney, 1986), which pose ATP demands associated with protein synthesis and repair (Hachiya, Terashima, & Noguchi, 2007) and functional linkages between photosynthetic and respiratory metabolism (Noguchi & Yoshida, 2008). Although R_{dark} scales with N, LMA, and $V_{\text{c,max}}$, and these three parameters can each be predicted with various levels of confidence from hyperspectral reflectance, we are aware of only one publication predicting R_{dark} directly from reflectance spectra (see Doughty et al., 2011). There might be limitations in prediction of a flux such as R_{dark} from reflectance spectra compared with prediction of capacity of other physiological processes, for example, $V_{\text{c,max}}$. This might be because R_{dark} is a physiological process driven by enzymatic reactions that dynamically adjust to short-term (seconds to minutes) and long-term (hours to days) environmental changes, whereas the proteins underpinning metabolic capacity can be more stable over time. In addition, respiratory enzymes may not exhibit distinct reflectance signatures that would enable direct quantification as such. Estimation of leaf R_{dark} may arise indirectly through secondary correlations with other leaf traits, for example, leaf N and LMA, as already discussed for $V_{\text{c,max}}$ ²⁵ (Dechant et al., 2017). Here, we investigate the possibility that variations in R_{dark} can be well predicted from hyperspectral signatures.

Appropriate analytical tools for assessing plant traits using hyperspectral reflectance data include partial least square regression (PLSR; Wold, Sjöström, & Eriksson, 2001), which combines features from principal component analysis and multiple regression, and machine learning algorithms such as support vector machine regression (SVMR; Vapnik, 1995). One of the most commonly used analytical tools in estimating plant traits from hyperspectral reflectance of leaves is PLSR. Doughty et al. (2011) used PLSR to predict R_{dark} from leaf hyperspectral reflectance collected from 149 species ($r^2 = 0.48$, RMSE = $-0.52 \mu\text{mol m}^{-2} \text{s}^{-1}$; and for canopy R_{dark} $r^2 = 0.16$, RMSE = $0.58 \mu\text{mol m}^{-2} \text{s}^{-1}$). This encouraged us to see if the method could be applied to wheat leaves.

To test the suitability of estimating leaf R_{dark} from hyperspectral reflectance data, three experiments were conducted during which

we characterized leaf R_{dark} , hyperspectral reflectance, biochemical (N content) and morphological (LMA) traits under different environmental conditions and plant growth stages, using a diverse set of wheat (*Triticum aestivum* L.) genotypes. We report on leaf respiration rates and associated leaf traits of 1380 samples from 90 genotypes. The varied conditions, growth stages, and genotypes were used to generate a wide range of R_{dark} values to robustly test different modelling approaches. We used two independent analytical tools (PLSR and SVMR) to investigate if:

1. Leaf R_{dark} can be well predicted from leaf hyperspectral reflectance data.
2. Model predictions of leaf R_{dark} from spectral reflectance data can be improved by using an alternative to PLSR, that is, SVMR.

Our study also provided an opportunity to assess the extent of genotypic and environment-driven variation in leaf respiration rates of commercial elite wheat lines, and the extent to which other traits such as leaf N and LMA are predictors of wheat leaf R_{dark} values.

2 | MATERIALS AND METHODS

Three independent experiments were conducted to explore associations (or the absence thereof) between leaf reflectance spectra and leaf R_{dark} in wheat. Two of the experiments (Experiments 1 and 2) were undertaken in climate-controlled glasshouses at the Australian National University (ANU), Canberra, whereas a third (Experiment 3) was conducted in a field-based polytunnel at CSIRO Ginninderra Experiment Station. Leaves of a diverse set of wheat genotypes (between 3 and 70 per experiment, see Table S1 for list of genotypes) were examined at different growth stages and under varied environmental conditions (Table 1). The varied growth stages and environmental conditions were used to generate a wide range of R_{dark} values and to ensure a robust test of our approach of using leaf reflectance spectra to predict leaf R_{dark} .

TABLE 1 Materials and growth environment for the different experiments

Experiment	Location	Genotypes ^a	Zadoks growth scale ^b	Leaf sampled	Day/night temperature (°C)	Light (PPFD, $\mu\text{mol m}^{-2} \text{s}^{-1}$), photoperiod
1	ANU ^c	3	13	Third true leaf (Leaf-3)	21/16, 28/23, or 35/30	600–800 or 150–200, 12 hr
2	ANU ^c	70	13 and 61–69	Leaf-3, leaf subtending the flag leaf (Flag-1) and flag leaf	25/20	400–1200, 10–12 hr day ⁻¹
3	CSIRO ^d	24	23–27 and 55–71	Leaf subtending Flag-1, Flag-1, and flag leaf	27/12	---, 12–14 hr day ⁻¹

Note. PPFD: photosynthetic photon flux density; ---: data not available.

^aA list is provided in Table S1.

^bZadoks et al. (1974).

^cGlasshouse at Controlled Environment Facilities, Research School of Biology, Australian National University, Canberra, Australia.

^dPolytunnel at CSIRO Ginninderra Field Station, North Canberra, Australia.

2.1 | Glasshouse Experiment 1—Exploring environment-induced variation in leaf respiration

Experiment 1 was carried out at the ANU Controlled Environment Facilities, Canberra, Australia. Three wheat genotypes, “Calingiri,” “Halberd,” and “Janz,” were selected to represent a wide range of average rates of R_{dark} ; an earlier study screening 138 lines (grown in controlled environment cabinets) showed twofold genotypic variation in R_{dark} among the wheat lines, with Calingiri, Halberd, and Janz being at high ($0.79 \mu\text{mol O}_2 \text{ m}^{-2} \text{ s}^{-1}$), mid ($0.50 \mu\text{mol O}_2 \text{ m}^{-2} \text{ s}^{-1}$), and low ($0.35 \mu\text{mol O}_2 \text{ m}^{-2} \text{ s}^{-1}$) range of R_{dark} values, respectively (Scafaro et al., 2017). Seeds were germinated on moist filter papers on March 9, 2016, with >95% germination achieved within 2 days. Five days after germination (DAG; on March 16, 2016), seeds were transferred into 2 L plastic pots (one seedling per pot) filled with Martins mix (Martins Fertilizers Ltd, Yass, NSW Australia). The potting mix was treated at 63°C for 1 hr prior to filling pots. The mix was enriched with Osmocote® OSEX34 EXACT slow-release fertilizer (Scotts Australia, Bella Vista, NSW, Australia). The base of the plastic pots was perforated in several places to ensure proper drainage upon watering. Seedlings were watered twice daily, in the morning and late afternoon, to avoid water deficit stress. The glasshouse was maintained at 12/12 hr day/night temperature of 28/23°C and ambient light condition. One-week-old seedlings were transferred to different treatments as per the experimental design described below.

The experimental design was a split-split plot with temperature, light, and genotype, respectively as main, sub, and sub-sub plots, replicated six times. There were three growth temperatures (12/12 hr day/night conditions of 21/16, 28/23, and 35/30°C), two light intensities (photosynthetic photon flux density of 600–800 $\mu\text{mol m}^{-2} \text{ s}^{-1}$ [high light] and 150–200 $\mu\text{mol m}^{-2} \text{ s}^{-1}$ [low light, that is, 25% of high light]), and three genotypes (Calingiri, Halberd, and Janz). The temperature regimes were maintained by automated heating and cooling systems. Changes in temperature occurred at 0700/1900 hr. The prevailing ambient light was taken as high light and to achieve low light a green mesh was placed over bespoke cages within which plants were kept (see Figure S1). This mesh and cage arrangement resulted in a 75% reduction of ambient light reaching the plants. Photoperiod during that time of the year was ~12 hr day⁻¹. Plants were kept under these conditions for 3 weeks, at the end of which plants were approximately at growth stage Z13 (seedling growth; Zadoks, Chang, & Konzak, 1974). The most recently expanded leaf (the third true leaf and henceforth designated as Leaf-3) was measured at 35 and 36 DAG; the first three replicates at 35 DAG and the rest at 36 DAG. We used 108 plants/leaf samples for Experiment 1.

2.2 | Glasshouse Experiment 2—Variation in leaf respiration among 70 genotypes

Experiment 2 was conducted in the same glasshouse facility as Experiment 1. Seeds of 70 wheat genotypes (see Table S1 for list of genotypes), a subset of the 138 genotypes used recently to validate a

technique for high-throughput measurement of R_{dark} (Scafaro et al., 2017), were used. The seeds were germinated and transferred into 2 L plastic pots filled with Martins mix as in Experiment 1. Seedlings were transferred on June 9, 2016 (six DAG). Plant nutrition and watering were as described for Experiment 1. The glasshouse was maintained for three consecutive months at 12/12 hr day/night temperature of 25/20°C with temperature changes at 0700/1900 hr. Light measured as photosynthetic photon flux density at plant height varied between 400 and 1200 $\mu\text{mol m}^{-2} \text{ s}^{-1}$ and photoperiod during this experiment was 10–12 hr day⁻¹.

The experimental design was a randomized complete block design with four replicates. Due to space limitations, the four replicates were split equally between two adjoining rooms in a glasshouse. Each replicate, consisting of 70 genotypes, was placed on a bench in a glasshouse ($n = 280$ plants). Each glasshouse room had a pair of benches. Leaf measurements were taken first at growth stage Z13 (seedling growth; 24–27 DAG) from Leaf-3 and then at growth stages Z61–69 (anthesis) from the leaf subtending the flag leaf (henceforth designated as Flag-1; 67–70 DAG) and the flag leaf (81–85 DAG). For each growth stage, measurements and sample collection were completed within 4–5 days. Each of the four replicates required at least 1 day for data collection. Total leaf samples used for Experiment 2 were 840.

2.3 | Poly tunnel Experiment 3—Variation in leaf respiration among 24 wheat genotypes

Seeds of 24 wheat genotypes (selected based on similarities in phenology—height and days to anthesis, but contrasting for $V_{\text{c,max}}$ and R_{dark}) were used for this experiment. Seeds were sown at a rate of 250 grains m^{-2} on September 16, 2016, in field plots, under a polytunnel, at CSIRO Ginninderra Experiment Station, Australian Capital Territory (35° 12'S, 149° 06'E; 600 m asl). The soil was a yellow chromosol (Isbell, 2002). Mean daily maximum/minimum air temperature obtained from a weather station installed in a neighbouring polytunnel from November to December was 27/12°C. A 30-year (1981–2010) average over the same period was 25/11°C, and from September to December was 22/8°C (data from the closest Bureau of Meteorology weather station). The photoperiod during the experiment was 12–14 hr day⁻¹. Plants were kept well-watered by drip irrigation and fertilized optimally. The experiment was laid out as a row \times column design with 12 rows and 6 columns, with each block containing two columns. As such, there were 72 plots, each block of 24 genotypes replicated three times. Each plot consisted of 10 equally spaced 1 m rows covering an area of 2.5 m^2 .

Measurements and sampling were at growth stages Z23–27 (tillering) and Z55–71 (inflorescence emergence, anthesis through milk development). At both growth stages, three sampling events were carried out on consecutive days. At growth stages Z23–27 (tillering), sampling and measurements were on the last fully expanded leaf, with one leaf measured from each plot each day for 3 days. The leaf sampled varied between Leaf-3 and the sixth true leaf (Leaf-6), when counting from the base of the plant. At growth stages Z55–71 (inflorescence

emergence, anthesis through milk development), the flag leaf and Flag-1 were sampled on the first and second day, respectively, whereas on the third day, the leaf subtending Flag-1 (designated as Flag-2) was sampled. In total, 432 leaf samples were collected for Experiment 3.

2.4 | Measured traits—All experiments

Reflectance spectra were captured from the adaxial surface of leaves using an ASD FieldSpec® 4 Full-Range spectroradiometer (Analytical Spectral Devices, Inc., Boulder, CO, USA) with spectral range 350–2500 nm and a rapid data collection time of 0.1 s per spectrum. Data from the full spectral range (350–2500 nm) was used for analysis. Spectral resolution of the device was 3, 10, and 10 nm (full width at half maximum) at 700, 1400, and 2100 nm, respectively. Sampling intervals were 1.4 and 2 nm for the spectral regions 350–1000 and 1000–2500 nm, respectively. The device was fitted with an ASD fibre optic cable and leaf clip. A mask attached to the leaf clip reduced the width of the aperture through which leaf reflectance was recorded to 11.5 mm, enabling easier measurement of leaf widths down to 12 mm (Silva-Pérez et al., 2018). Leaf spectral reflectance was captured between 1000 and 1400 hr from the adaxial surface and close to the midpoint of the leaf. Each leaf was measured at one position, taking less than 20 s. An internal light source was used to illuminate a white reference panel for calibration or a leaf placed in front of a black panel during measurement. After measuring the reflectance spectrum, the leaf was immediately detached near the ligule for subsequent measurement of R_{dark} . Samples were temporarily stored in zip lock bags with moist tissue paper or cotton balls and placed in Styrofoam boxes partly filled with ice blocks/packs for transfer from glasshouse/field to the laboratory. R_{dark} values were determined within 24 hr of obtaining spectral reflectance values. Leaf sections of $\sim 4 \text{ cm}^2$, including the exact spot where the reflectance measurement was taken from, were dissected from the whole leaf and used for determination of other traits.

The dissected leaf section was weighed and exact area determined. The $\sim 4 \text{ cm}^2$ leaf sections were placed in an automated Q2 O_2 -sensor (Astec Global, Maarssen, The Netherlands) to determine O_2 consumption rate following the method of Scafaro et al. (2017). Briefly, freshly dissected leaf tissues were placed in 2 ml tubes and hermetically sealed with specialized caps (Astec Global). The top surfaces of caps contained a fluorescent metal organic dye, sensitive to O_2 quenching. The tubes were loaded onto racks, which individually accommodated 48 tubes, and racks placed on the Q2 O_2 -sensor. Each rack was loaded with two tubes filled with ambient air (designated 100% O_2) and N_2 (designated as 0% O_2), for calibration of the Q2 O_2 -sensor before measurement was made. An automated robotic arm with fibre optic fluorescence detection capability scanned the rows of tubes enabling the quantification of O_2 dependent decay in fluorescence signal. The percent O_2 relative to the air calibration tube was converted to absolute values of R_{dark} in moles of $\text{O}_2 \text{ s}^{-1}$. The Q2 O_2 -sensor was set at 25°C and measurements taken at a frequency of 4 min over a 2 hr period. However, values from the first 30 min were disregarded, as

they tend to be unstable—respiratory activity rapidly increased and decreased during this period (Scafaro et al., 2017).

All leaf samples used for determination of R_{dark} were oven dried at 70°C for 48 hr (Experiments 1 and 2) or 60°C for 72 hr (Experiment 3), and then, LMA was determined. The same samples were then used to determine leaf N content (%), by combustion using a Carlo-Erba elemental analyser (NA1500, Thermo Fisher Scientific, Milan, Italy). Area, fresh mass, dry mass, and N content (per gram of leaf dry mass, N_{mass} , or per square metre of leaf area, N_{area}) of the leaf section used for determination of R_{dark} were used to calculate R_{dark} per (a) square metre of leaf area ($R_{\text{dark_LA}}$, $\mu\text{mol O}_2 \text{ m}_{\text{LA}}^{-2} \text{ s}^{-1}$); (b) gram of leaf fresh mass ($R_{\text{dark_FM}}$, $\text{nmol O}_2 \text{ g}_{\text{FM}}^{-1} \text{ s}^{-1}$); (c) gram of leaf dry mass ($R_{\text{dark_DM}}$, $\text{nmol O}_2 \text{ g}_{\text{DM}}^{-1} \text{ s}^{-1}$); and (d) gram of leaf N_{mass} ($R_{\text{dark_N}}$, $\text{nmol O}_2 \text{ g}_{\text{N}}^{-1} \text{ s}^{-1}$).

2.5 | Model development for prediction of leaf traits from reflectance spectra

Different regression techniques, including PLSR and SVMR, have been used to quantify relationships between spectral data and leaf/canopy traits. But only PLSR has been used to predict leaf/canopy R_{dark} of 149 species (for prediction of leaf R_{dark} $r^2 = 0.48$, RMSE = $-0.52 \mu\text{mol}\cdot\text{m}^{-2}\cdot\text{s}^{-1}$; and for canopy R_{dark} $r^2 = 0.16$, RMSE = $0.58 \mu\text{mol}\cdot\text{m}^{-2}\cdot\text{s}^{-1}$; Doughty et al., 2011), although not including wheat. The SVMR is considered a powerful regression technique (Thissen, Pepers, Üstün, Melssen, & Buydens, 2004), in terms of model performance and prediction accuracy. Therefore, we independently tested the different models for leaf traits using these two regression techniques.

Prior to data analysis, a multiplicative correction module (ASD Spectral Analysis and Management System [SAMS®] version 3.2) was applied to the reflectance data at 1000 and 1800 nm to correct for “jumps” observed in apparent reflectance at the intersections between different detector ranges. As did Silva-Pérez et al. (2018), reflectance spectra with values greater than 0.7 between 800 and 1000 nm were treated as an outlier and removed.

Variation in foliar traits (including R_{dark}) and biochemical composition based on leaf optical properties were modelled using PLSR and SVMR. The PLSR technique could be performed with either the continuous full-spectrum data (Asner & Martin, 2008) or a predetermined spectral subset (Bolster, Martin, & Aber, 1996). We initially applied the PLSR model building approach of Serbin et al. (2012) and Wold et al. (2001) to 90% of the dataset (training dataset). This works by extracting latent variables (i.e. underlying factors or indices produced by the observable variables that account for most of the variation in the response) from sampled factors and responses. This step is analogous but not identical to principal component regression. Then, the extracted factors are applied in a set of regression equations and used to construct predictions of the responses. PLSR models can suffer from overfitting if the number of model components selected is sub-optimal. To avoid overfitting, we selected the optimal number of model components for the PLSR model by minimizing the root mean squared error of prediction. The root mean squared error of prediction was calculated by k-fold cross validation. The optimal PLSR model was

subsequently applied to estimate measured traits of the remaining 10% of dataset (test dataset). This was done independently for each trait of interest.

Like our PLSR model, we initially built the SVMR model on 90% of the dataset (training dataset) then subsequently used the built model to estimate measured traits of the remaining 10% (test dataset). To develop our SVMR models, we used the epsilon-regression form of SVMR and followed the recommendation of Hsu, Chang, and Lin (2003). We chose the Gaussian (radial basis function) kernel type for our model. The radial basis function is a general purpose kernel used when there is no prior knowledge about the data. Then, we combined this with a k-fold ($k = 10$) cross validation approach that optimized for model cost parameter (C) and kernel parameter (γ). Cost and kernel parameters resulting in the best model fit, that is, highest squared Pearson correlation (r^2) on the training dataset, were selected. This was then used to calculate validation statistics for the test dataset (the remaining 10% of dataset not used for model building).

PLSR and SVMR analyses were carried out in the R statistical environment (R Core Team, 2018) using the packages “pls” (Mevik, Wehrens, & Liland, 2016) and “e1071” (Meyer, Dimitriadou, Hornik, Weingessel, & Leisch, 2017), respectively. Model predictions for 90/10 training/test datasets were compared for PLSR and SVMR and for all three experiments combined based on their r^2 , RMSE, and relative bias (%). In addition, we undertook model validation by predicting R_{dark} of individual or combined experiments using hyperspectral-based models built on individual experiments or various combinations of experiments.

2.6 | Statistical analysis

Leaf R_{dark} , N , and LMA were subjected to analysis of variance after tests for normality (Bartlett's test and visual assessment of Q-Q plot) and homogeneity of variances (Shapiro-Wilk's test and plots of residuals against fitted values). Outliers were identified and removed from the dataset using the Tukey's method; that is, values above and below the $1.5 \times \text{IQR}$ (the interquartile range) were removed. Tukey's method

was chosen over the standard deviation method because it is independent of the distribution of the data and is resistant to extreme values.

3 | RESULTS

3.1 | Leaf reflectance spectral properties

Leaf reflectance spectra varied substantially within and between experiments (Figures 1 and S2). For example, reflectance at 400 nm ranged between 0.04–0.07 (Experiment 1), 0.03–0.11 (Experiment 2), and 0.03–0.17 (Experiment 3, Figure S2). Across all experiments, the largest range in leaf reflectance was in the NIR region. However, the coefficient of variation (CV) of reflectance for this region was the least (23%) compared with 33% for the SWIR and 32% for the visible regions. The wavelengths with the largest and smallest range of reflectance were 1926 (79%) and 1076 nm (21%), respectively.

3.2 | Variation in leaf traits

Leaf $R_{\text{dark_LA}}$, $R_{\text{dark_FM}}$, and $R_{\text{dark_DM}}$ across experiments were on average $0.73 \mu\text{mol O}_2 \text{ m}_{\text{LA}}^{-2} \text{ s}^{-1}$, $4.05 \text{ nmol O}_2 \text{ g}_{\text{FM}}^{-1} \text{ s}^{-1}$, and $21.1 \text{ nmol O}_2 \text{ g}_{\text{DM}}^{-1} \text{ s}^{-1}$, respectively, showing a sevenfold to ninefold variation (Table 2). Leaf $R_{\text{dark_N}}$ averaged $449 \text{ nmol O}_2 \text{ g}_{\text{N}}^{-1} \text{ s}^{-1}$ spanning a 15-fold range of values ($87\text{--}1260 \text{ nmol O}_2 \text{ g}_{\text{N}}^{-1} \text{ s}^{-1}$). The large range in $R_{\text{dark_N}}$ compared with other traits was also characterized by ~25% higher CV than $R_{\text{dark_LA}}$, $R_{\text{dark_FM}}$, or $R_{\text{dark_DM}}$ (CV = 0.37 for $R_{\text{dark_N}}$ vs. 0.28–0.29 for others; Table 2). Leaf N_{mass} averaged 49.5 mg g^{-1} (CV = 0.28), N_{area} 0.87 g m^{-2} (CV = 0.21), and LMA 31.5 g m^{-2} (CV = 0.29) with twofold to fivefold variation (Table 2). Table 2 provides a summary of leaf traits for each and all experiments combined. Treatment or leaf level summaries and analysis of variance results for Experiments 1, 2, and 3 are provided in Tables S2, S3, and S4, respectively. Broadly, rates of R_{dark} were affected by growth irradiance, with markedly lower rates in plants grown under low light compared with those under high light, with inconsistent effects of growth temperature R_{dark} (measured at 25°C ; Table S2). Growth stage was also found to have strong effects on R_{dark} , albeit with the differences

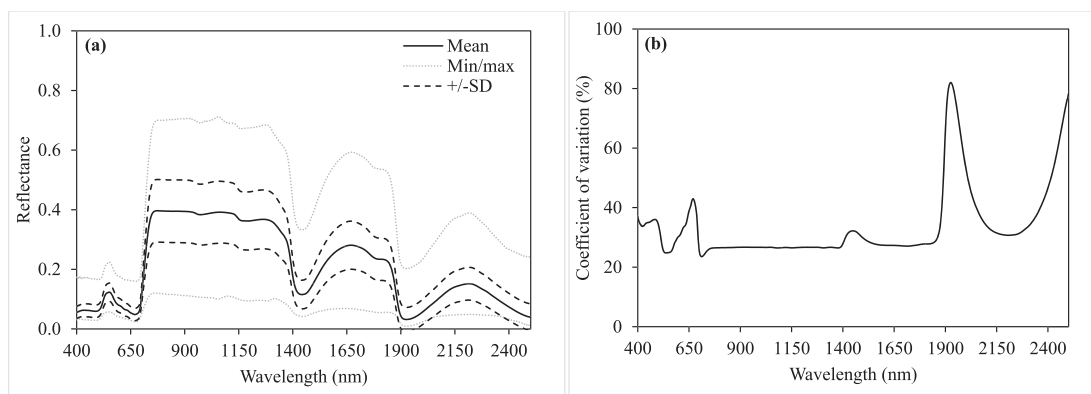


FIGURE 1 Mean (\pm standard deviation), minimum and maximum leaf reflectance (a) of wheat and spectral coefficients of variation (b) for three experiments (Experiments 1, 2, and 3) combined

TABLE 2 Variation in leaf dark respiration (R_{dark} , per square metre of leaf area [LA], per gram of fresh mass [FM], dry mass [DM], or leaf nitrogen [N]), nitrogen (per gram of DM, N_{mass} , or per square metre of LA, N_{area}), and leaf mass per area (LMA) of wheat genotypes

Trait	Experiment 1		Experiment 2		Experiment 3		All experiments Mean (CV)
	Range	Mean \pm SD	Range	Mean \pm SD	Range	Mean \pm SD	
Leaf R_{dark} per unit							
LA ($\mu\text{mol O}_2 \text{ m}_{\text{LA}}^{-2} \text{ s}^{-1}$)	0.18–1.04	0.50 \pm 0.18	0.28–1.27	0.72 \pm 0.18	0.26–1.27	0.83 \pm 0.21	0.73 (0.28)
FM ($\text{nmol O}_2 \text{ g}_{\text{FM}}^{-1} \text{ s}^{-1}$)	0.82–5.24	2.62 \pm 0.88	1.66–7.33	4.10 \pm 1.07	1.19–7.25	4.30 \pm 1.12	4.05 (0.29)
DM ($\text{nmol O}_2 \text{ g}_{\text{DM}}^{-1} \text{ s}^{-1}$)	5.26–32.05	17.96 \pm 4.61	7.66–37.38	22.37 \pm 6.09	5.17–35.40	19.22 \pm 5.67	21.05 (0.29)
N ($\text{nmol O}_2 \text{ g}_{\text{N}}^{-1} \text{ s}^{-1}$)	86.6–540.4	293.7 \pm 86.4	149.4–675.6	403.7 \pm 85.2	144.0–1,260.5	599.5 \pm 226.4	448.5 (0.37)
Other leaf traits							
N_{mass} (mg g^{-1})	53.8–71.3	61.8 \pm 3.5	33.6–77.1	55.8 \pm 10.2	17.3–64.6	34.1 \pm 7.8	49.5 (0.28)
N_{area} (g m^{-2})	0.50–1.41	0.86 \pm 0.20	0.48–1.44	0.94 \pm 0.17	0.32–1.44	0.74 \pm 0.23	0.87 (0.21)
LMA (g m^{-2})	16.9–41.7	27.0 \pm 6.2	17.2–57.8	33.0 \pm 7.8	14.2–59.0	29.7 \pm 11.6	31.5 (0.29)

Note. CV: coefficient of variation; SD: standard deviation; $n = 105$ – 107 , 815 – 840 , and 398 – 423 for Experiments 1, 2, and 3, respectively.

between vegetative and reproductive varying depending on the units that R_{dark} was expressed (Tables S3 and S4).

3.3 | Correlations of leaf respiration with other leaf traits

Correlations of R_{dark} with leaf N and LMA were poor (r between -0.08 and 0.38), irrespective of the units that rates were expressed in (Figure 2 and Table 3), with the exception being between R_{dark_N} and leaf N_{mass} ($r = -0.59$). See Figure S3 for more detailed results of individual experiments. The signs of the correlations of R_{dark} with leaf N_{mass} and LMA differed, with R_{dark} having a negative association with leaf N_{mass} , except for $R_{\text{dark}_{DM}}$, whereas R_{dark} had a positive association with LMA, except for $R_{\text{dark}_{DM}}$. Leaf N_{mass} , N_{area} , and LMA correlated significantly ($P < 0.001$) with one another albeit poorly ($r = 0.12$ – 0.49 ; Figure 3, Table 3). Also, see Figure S4 for individual experiments.

3.4 | Predictions of leaf respiration and other traits based on a subset of pooled experimental data (10% test dataset)

We validated our models using a test dataset that consisted of 10% of our pooled experimental data, which was not used in building the models. Across experiments, predictions of leaf R_{dark} varied per unit leaf area, DM and N ($r^2 = 0.50$ – 0.63 for PLSR, Figure 4 and $r^2 = 0.53$ – 0.64 for SVMR, Table 4). Values of r^2 were generally highest for R_{dark} per leaf N and least when expressed per gram of leaf dry mass (Table 4). Relative bias were between 16% and 18% (Table 4). Model predictions of leaf N_{mass} , N_{area} , and LMA achieved r^2 of 0.91, 0.60, and 0.75, respectively, with PLSR (Figure 5). For SVMR, predictions of N_{mass} , N_{area} , and LMA had r^2 of 0.90, 0.79, and 0.72, respectively. The corresponding relative bias were 7–12% for PLSR and 8–11% for SVMR.

3.5 | Comparison of PLSR and SVMR

Performance of the PLSR model was comparable with that using SVMR, with similar r^2 and RMSE, and differences in relative bias under 2% (Table 4). A similar result (i.e. no clear indication that SVMR outperformed PLSR) was obtained using a multimethod ensemble developed by Feilhauer, Asner, and Martin (2015) and tested on either the continuous full spectrum data or a spectral subset that was selected based on weightings (Table S5; also see Text S1 for our attempt to reduce model complexity and improve prediction using the multimethod ensemble of Feilhauer et al., 2015). The presentation of further results will therefore be limited to those from PLSR models using the full spectral range.

3.6 | Cross-predictions of leaf respiration and other traits of experimental data

PLSR models built on one experiment were poor at predicting R_{dark} of a different experiment (Figures 6 and S5). The best outcome was predicting $R_{\text{dark}_{LA}}$ for Experiment 1 using a model developed from Experiment 2 ($r^2 = 0.33$). Similarly, models built on single glasshouse experiments were poor at predicting that of the field experiment and vice versa. The best r^2 for this method was 0.21, for a model built from Experiment 3 predicting $R_{\text{dark}_{DM}}$ for glasshouse Experiment 2. By contrast, predictions of R_{dark} based on models built on a combination of Experiments 1 and 2 or all three experiments were better than or similar to models built on one experiment (Figures 6 and S5). For example, a model developed on 90% of data comprising all three experiments predicted (i.e. was validated on) $R_{\text{dark}_{DM}}$ of the remaining 10% of data for each of Experiments 1, 2, and 3 with r^2 of 0.20, 0.66, and 0.61, respectively. This compares to r^2 of 0.04, 0.61, and 0.45 when models were built with 90% of data solely from same experiment and validated on the remaining 10%. Similar results were obtained with N_{area} (Figures 7 and S6).

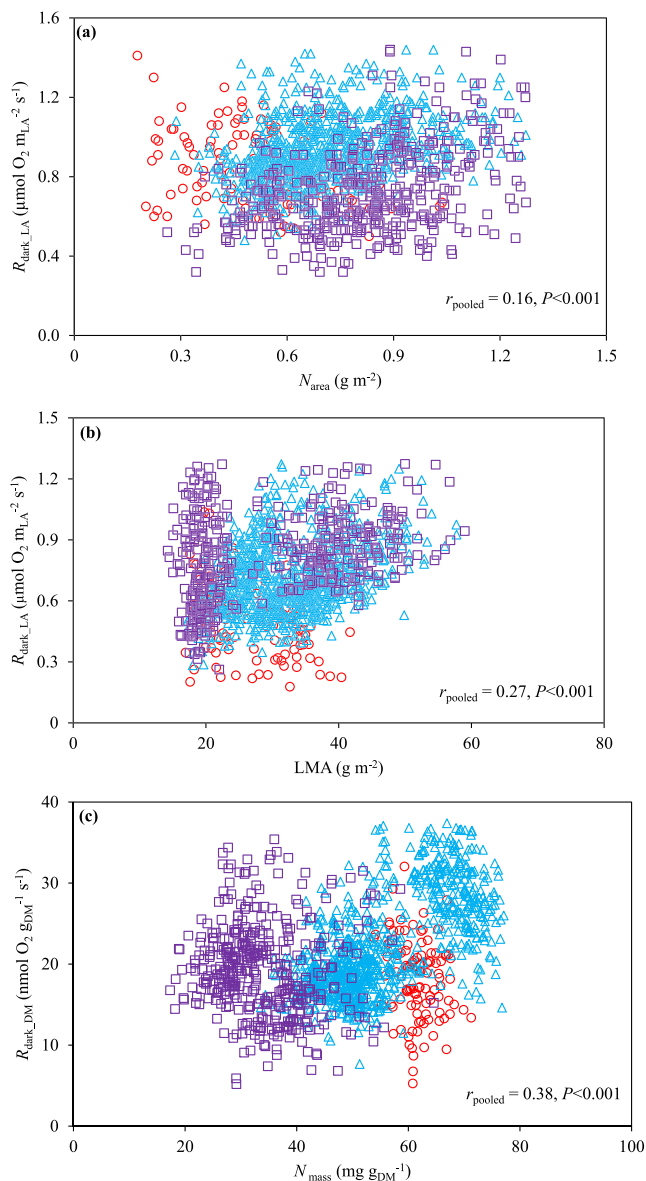


FIGURE 2 Relationships between $R_{\text{dark_LA}}$ and (a) nitrogen content per unit leaf area (N_{area}), (b) leaf dry mass per unit leaf area (LMA), and (c) between $R_{\text{dark_DM}}$ and nitrogen concentration per unit leaf dry mass (N_{mass}). Pearson correlation coefficients (r) for data pooled from Experiments 1, 2, and 3 are presented in the plots. For each of Experiment 1 (red circles), Experiment 2 (blue triangles), and Experiment 3 (purple squares), the respective r were -0.36 , 0.36 , and 0.40 for $R_{\text{dark_LA}}$ versus N_{area} , -0.37 , 0.33 , and 0.33 for $R_{\text{dark_LA}}$ versus LMA, and -0.20 , 0.63 , and -0.10 for $R_{\text{dark_DM}}$ versus N_{mass}

4 | DISCUSSION

Our study has produced a large dataset of wheat leaf R_{dark} rates (1380 samples), obtained from 90 genotypes, multiple growth stages and grown under varying environmental conditions. We show that leaf R_{dark} can be predicted from reflectance spectra with model r^2 values of 0.50–0.63 and relative bias of 17–18%. PLSR model

predictions of leaf R_{dark} from spectral reflectance data were as good as SVMR. Models predicting R_{dark} from leaf reflectance spectra generally performed better when trained on more diverse data, such as genotype, growth stage, and growing conditions. Our ability to predict R_{dark} from reflectance spectra could arise from (a) indirect association with other traits (e.g. N_{area} , N_{mass} , and LMA); (b) links with spectral signatures of key photosynthetic components such as $V_{\text{c,max}}$ and/or J_{max} whose variations are coupled with variations in R_{dark} ; and (c) spectral absorption features by respiratory substrates or components in the respiratory system. These possibilities are discussed in detail in Section 4.2.

4.1 | Variation in wheat leaf respiration and other leaf traits

Wheat leaf R_{dark} varied enormously, irrespective of how it was expressed. The sevenfold variation in wheat leaf $R_{\text{dark_LA}}$ reported here is higher than the modest twofold reported by Scafaro et al. (2017) for wheat and by O'Leary et al. (2017) for *Arabidopsis* (*Arabidopsis thaliana* L.). It is comparable with the tenfold variation for 899 species covering plant functional types from the Arctic to the tropics (Atkin et al., 2015). Variations reported here for wheat leaf N and LMA were in line with other reports for wheat (Ecartot et al., 2013; Martin et al., 2018), other crops (Jullien, Allirand, Mathieu, Andrieu, & Ney, 2009), and within natural ecosystems (Asner et al., 2014; Wright et al., 2004). These variations were caused by genotypic, growth, and environmental effects. For instance, the plot of leaf $R_{\text{dark_DM}}$ versus N_{area} (Figure 2c) showed distinct clusters of the vegetative and reproductive stages of both Experiments 2 and 3. Also, the plot of $R_{\text{dark_LA}}$ versus N_{area} (Figure 2a) could be distinguished by Experiment, with higher $R_{\text{dark_LA}}$ per leaf N_{area} for Experiment 2 compared with Experiment 3. The higher leaf R_{dark} per leaf N_{area} during growth stages Z13/Z23–27 (i.e. seedling growth/tillering) of Experiments 2 and 3 or of some genotypes compared with others suggests greater relative allocation of leaf N to metabolic processes than to structural properties (Evans, 1989a, 1989b; Harrison, Edwards, Farquhar, Nicotra, & Evans, 2009), higher demand for respiratory products, and/or increase in ATP turnover (Atkin & Tjoelker, 2003; O'Leary et al., 2017).

In natural ecosystems and even within species, individual plants experiencing cold growth conditions can exhibit higher temperature-normalized rates of leaf R_{dark} than individuals of the same genotypes growing in warmer habitats (Atkin, Scheurwater, & Pons, 2006; Mooney, 1963; Oleksyn et al., 1998; Xiang, Reich, Sun, & Atkin, 2013). Cooler growth temperatures can induce increases in density and ultrastructure of mitochondria (Armstrong, Logan, & Atkin, 2006; Armstrong, Logan, O'Toole, Tobin, & Atkin, 2006; Miroslavov & Kravkina, 1991) and increase capacity of individual mitochondria (Armstrong, Logan, O'Toole, et al., 2006), both potentially contributing to the variation in leaf R_{dark} . However, variations in leaf R_{dark} and other leaf traits reported in this study were likely in response to a combination of factors, in addition to temperature. Other factors such as growth irradiance and evaporative demand that differed among the

TABLE 3 Pearson correlation coefficients matrix for leaf dark respiration (R_{dark} , per square metre of leaf area [LA], per gram of fresh mass [FM], dry mass [DM], or leaf nitrogen [N]), nitrogen (per gram of DM, N_{mass} , or per square metre of LA, N_{area}), and leaf mass per area (LMA) of all three experiments

Trait	Leaf R_{dark} per unit					
	LA ($\mu\text{mol O}_2 \text{ m}_{\text{LA}}^{-2} \text{ s}^{-1}$)	FM ($\text{nmol O}_2 \text{ g}_{\text{FM}}^{-1} \text{ s}^{-1}$)	DM ($\text{nmol O}_2 \text{ g}_{\text{DM}}^{-1} \text{ s}^{-1}$)	N ($\text{nmol O}_2 \text{ g}_{\text{N}}^{-1} \text{ s}^{-1}$)	N_{mass} (mg g^{-1})	N_{area} (g m^{-2})
R_{dark} per unit LA						
R_{dark} per unit FM	0.881***					
R_{dark} per unit DM	0.529***	0.451***				
R_{dark} per unit N	0.684***	0.587***	0.457***			
N_{mass}	-0.290***	-0.270***	0.377***	-0.592***		
N_{area}	0.159***	0.219***	0.178***	-0.307***	0.494***	
LMA	0.268***	0.347**	-0.080**	0.111***	-0.230***	0.118***

Note. Values are Pearson's r .

* $P < 0.05$. ** $P < 0.01$. *** $P < 0.001$

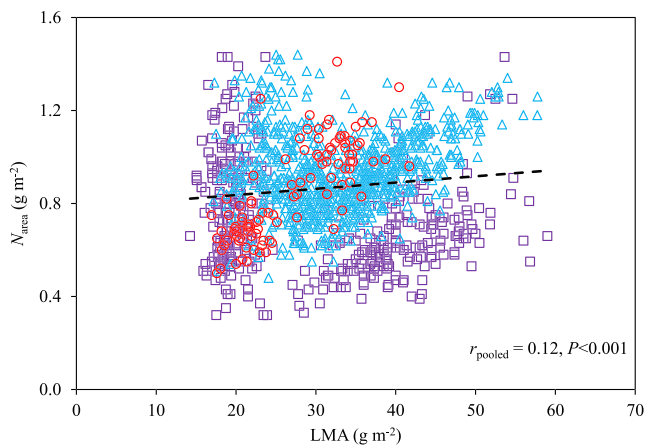


FIGURE 3 Relationship between nitrogen content per unit leaf area (N_{area}) and leaf dry mass per unit leaf area (LMA) for all three experiments combined. Pearson correlation coefficients (r) for each of Experiment 1 (red circles), Experiment 2 (blue triangles), and Experiment 3 (purple squares) were 0.78, 0.22, and -0.19, respectively. For all bivariate relationships between traits across all experiments, see Table 3

experiments and play key roles in moderating leaf R_{dark} , N, and LMA (Lusk, Reich, Montgomery, Ackerly, & Cavender-Bares, 2008; Poorter, Niinemets, Poorter, Wright, & Villar, 2009) may also have contributed.

4.2 | What underpins the ability to predict leaf respiration from leaf reflectance?

Hyperspectral reflectance characteristics of leaves have been used to predict LMA, leaf N, and photosynthetic traits. Extending this approach to predict R_{dark} seemed plausible given that R_{dark} scales with LMA (Wright et al., 2006), leaf N (Reich et al., 2008; Reich, Walters,

Ellsworth, et al., 1998; Ryan, 1991; Wright et al., 2004), and photosynthesis (Bouma, De Visser, Van Leeuwen, De Kock, & Lambers, 1995; O'Leary et al., 2017). Although the prediction of R_{dark} could in part be related to N or LMA, in our study, clear and simple correlations were not evident (Figure 2a,b). Predicting R_{dark} using multiple linear regression against N and LMA only achieved r^2 values up to 0.12 (Table S6) compared with 0.54 achieved with PLSR. Allocation of leaf N to respiratory proteins, respiratory energy needed for protein turnover, and utilization of N in building thicker and denser leaves all link R_{dark} to N and LMA. The weak relationship between R_{dark} , N, and LMA when R_{dark} and N are expressed on an area basis is not uncommon (Hirose & Werger, 1987; Reich, Walters, & Ellsworth, 1997; Reich, Walters, Ellsworth, et al., 1998; Wright et al., 2004). Similar weak relationships have sometimes been observed between CO_2 assimilation rate and N_{area} (Reich & Walters, 1994). We also found weak relationships between R_{dark} and N_{mass} , and between R_{dark} and LMA, which contrasts with the general literature dominated by interspecific studies (Reich, Walters, Ellsworth, et al., 1998; Wright et al., 2004). However, reported relationships for intraspecific studies have been mixed (Byrd, Sage, & Brown, 1992; Fan et al., 2017; Hirose & Werger, 1987). This indicates a weak coupling of N, protein content, and leaf structure to leaf R_{dark} within species such as wheat, which may be due to a range of factors, including the extent to which the genotypes differed in the degree of adenylate restriction (i.e. adenosine diphosphate (ADP) concentrations and ADP/ATP ratios) of mitochondrial electron transport (Hoefnagel & Wiskich, 1998).

Photosynthesis and R_{dark} are interrelated. The substrates for R_{dark} required to power processes such as protein turnover and phloem loading are provided by photosynthesis. Our ability to predict R_{dark} might be an indirect reflection of photosynthesis. Considering that the light saturated ambient rate of photosynthesis and the two major determinants of photosynthetic performance— $V_{\text{c,max}}$ and J_{max} —can also be predicted from leaf reflectance (Ainsworth et al., 2014; Barnes et al., 2017; Dechant et al., 2017; Doughty et al., 2011; Heckmann,

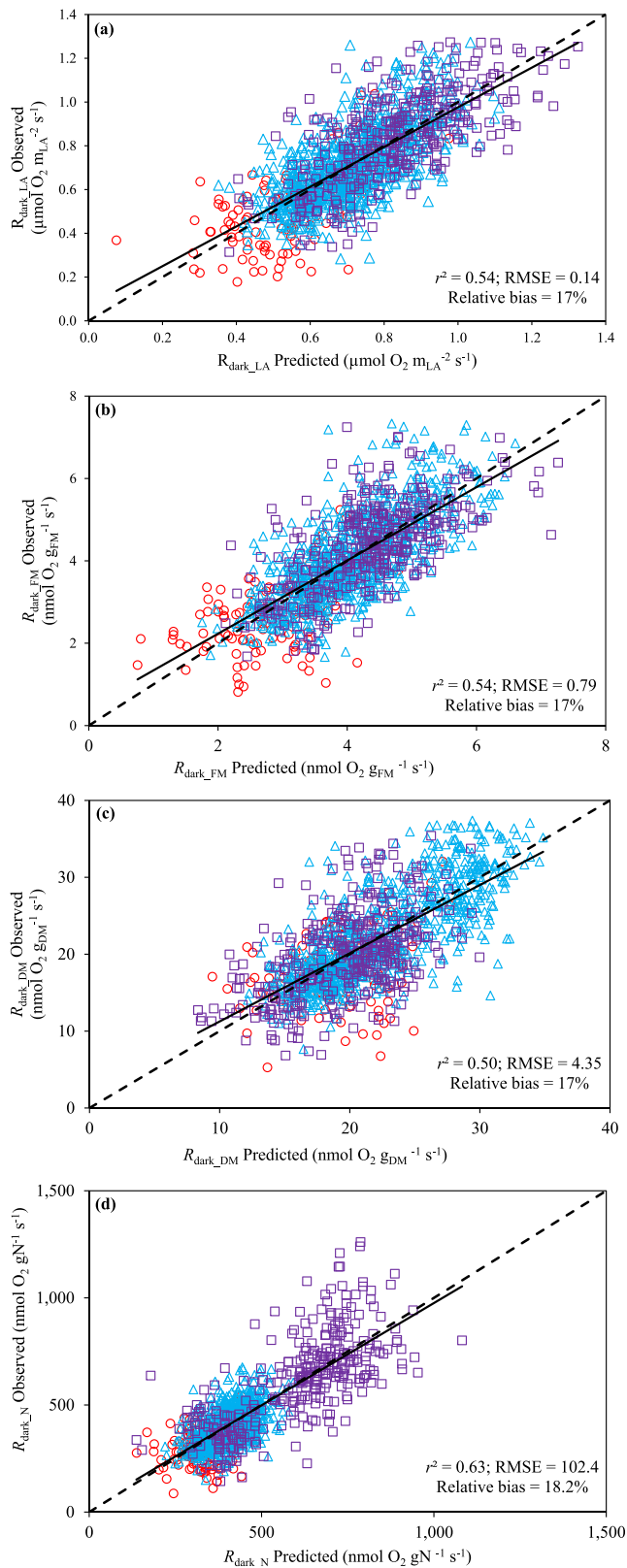


FIGURE 4 Validation of partial least square regression model prediction for $R_{\text{dark_LA}}$ (a), $R_{\text{dark_FM}}$ (b), $R_{\text{dark_DM}}$ (c), and $R_{\text{dark_N}}$ (d) using 10% of pooled data from Experiment 1 (red circles), Experiment 2, (blue triangles) and Experiment 3 (purple squares) that were not used in developing the model

Schlüter, & Weber, 2017; Serbin et al., 2012; Silva-Pérez et al., 2018; Yendrek et al., 2017), one possibility is that variations in R_{dark} are coupled to variations in $V_{c,\text{max}}$ and/or J_{max} and that the ability to predict R_{dark} from leaf reflectance is, in part, due to spectral signatures of key photosynthetic components. Dechant et al. (2017) reported that the prediction of $V_{c,\text{max}}$ ²⁵ from leaf reflectance is a secondary one, driven primarily by the prediction of leaf N. However, because the prediction of R_{dark} here for wheat using N_{area} , LMA, or their combination was poor (for $R_{\text{dark_LA}}$, highest $r^2 = 0.12$) compared with the PLSR model (see Table S6 for multiple regression results for $R_{\text{dark_LA}}$), our success in predicting R_{dark} indicates that there is additional information contained within the reflectance spectra associated with R_{dark} .

Spectral signatures associated with R_{dark} could be related to respiratory substrates or components in the respiratory system. These could include (a) the abundance of sugars, organic acids and adenylates (ATP and ADP); (b) abundance of respiratory enzymes with distinct spectral properties; or (c) aspects of mitochondrial mass or lipid composition. Both leaf starch and sugar content are correlated with R_{dark} (Noguchi, 2005; O'Leary et al., 2017; Peraudeau et al., 2015), and they have both been estimated from hyperspectral reflectance within the range reported in this study (Curran, 1989; Ramirez et al., 2015). Cytochrome c oxidase (COX) a respiratory protein complex in the mitochondrial respiratory chain also exhibits spectral characteristics (Appaix et al., 2000; Mason, Nicholls, & Cooper, 2014). Connections between O_2 consumption, COX, and spectral absorbance in vegetables have been shown (Makino, Ichimura, Kawagoe, & Oshita, 2007; Makino, Ichimura, Oshita, Kawagoe, & Yamanaka, 2010), but Umbach, Lacey, and Richter (2009) argued against a direct functional link between alternative oxidase (AOX, another respiratory protein) and floral reflectance, which probably also applies to leaf O_2 consumption, AOX, and reflectance. Another possibility is that the recent discovery of an association between mitochondrial functions and cell wall properties in plants (Hu et al., 2016) may indirectly link surface reflectance with respiratory processes. The reliability of our model prediction of R_{dark} ($r^2 = 0.50$ – 0.63) was considerably less than that for N ($r^2 = 0.91$), which probably represents the fact that R_{dark} is determined by a complex and varied array of components. Clearly, further research is required to understand the mechanistic basis underpinning leaf R_{dark} estimation from spectral reflectance signatures, possibly by using mutants, sampling at different times of the day, or treatments which alter photosynthetic capacity, levels of respiratory substrates and mitochondrial proteins.

4.3 | Model cross-prediction improved with data from other experiments

Our models, whether built on the whole spectrum (350–2500 nm) or a selected subset of wavelengths, gave good predictions of R_{dark} and other leaf traits for subsets of data not used to build the models. However, predictions of leaf traits for one experiment based on models built on a different experiment were poor (Figures 6, 7, S5,

TABLE 4 Summary of PLSR and SVMR model performance for prediction of leaf dark respiration (R_{dark} , expressed per square metre of leaf area [LA], per gram of fresh mass [FM], per gram dry mass [DM], and per gram leaf nitrogen [N]) and other target traits, including leaf nitrogen (expressed per gram of DM and per square metre of LA) and leaf mass per unit area (LMA) across all experiments

All experiment ^a	Coefficient of determination (r^2)		Root mean square error (RMSE)		Relative bias (%)	
	PLSR (NC ^b)	SVMR	PLSR	SVMR	PLSR	SVMR
R_{dark} LA ($\mu\text{mol O}_2 \text{ m}_{\text{LA}}^{-2} \text{ s}^{-1}$)	0.54 (23)	0.53	0.14	0.15	16.7	15.5
R_{dark} FM ($\text{nmol O}_2 \text{ g}_{\text{FM}}^{-1} \text{ s}^{-1}$)	0.55 (24)	0.53	0.79	0.80	17.0	18.1
R_{dark} DM ($\text{nmol O}_2 \text{ g}_{\text{DM}}^{-1} \text{ s}^{-1}$)	0.50 (23)	0.48	4.34	4.87	17.4	16.7
R_{dark} N ($\text{nmol O}_2 \text{ g}_{\text{N}}^{-1} \text{ s}^{-1}$)	0.63 (18)	0.64	102.4	103.8	18.2	17.0
N_{mass} (mg g^{-1})	0.91 (26)	0.90	4.15	4.35	7.1	8.0
N_{area} (g m^{-2})	0.60 (18)	0.62	0.13	0.13	11.8	11.1
LMA (g m^{-2})	0.75 (14)	0.72	4.53	5.05	11.3	10.8

Note. PLSR: partial least square regression; SVMR: support vector machine regression.

^aModels were built on training datasets consisting of 90% of the experimental data and used to predict the remaining (test dataset of) 10%.

^bNumber of components used.

and S6). Poor model performance across experiments is not uncommon. Silva-Pérez et al. (2018) reported that models derived from field-grown aspen leaves (*Populus tremuloides* Michx.; Serbin et al., 2012) gave poor predictions when applied to wheat leaves. The predictive performance of multivariate regression models may be increased by training models with more diverse data. For example, r^2 for Experiment 3 $R_{\text{dark_LA}}$ PLSR model, which was trained on just Experiment 3 data, was significantly lower than predictions of the same data using a model trained with data from all three experiments (Figure 6). Development of a system for adding novel data to an existing large spectral library for retraining models could prove to be a large cost-saving measure for large scale breeding trials and ecosystem management projects. This approach, called spiking, has been successfully applied in other fields such as soil biochemistry (Guerrero et al., 2014, 2016; Guerrero, Zornoza, Gómez, & Mataix-Beneyto, 2010). Further research is needed, however, to determine the minimum data from a novel source required to achieve good model predictions of traits.

4.4 | Machine learning approaches to improve model performance

To test if model prediction of R_{dark} could be improved by using alternatives to PLSR, we applied SVMR and compared the results with those from PLSR. Our comparison suggests model prediction was not limited by the use of PLSR. In addition, an independent comparison of PLSR with SVMR and random forest regression (RFR; Breiman, 2001) using a different modelling approach reported by Feilhauer et al. (2015), namely, a multimethod ensemble, which included PLSR, SVMR, and RFR, still showed PLSR was as good as the alternatives (Table S5; Text S1). Heckmann et al. (2017) carried out a similar comparison of model performance across a wider range of algorithms for predicting crop trait from leaf reflectance and preferred PLSR models because it yielded the highest predictive power.

The ensemble of Feilhauer et al. (2015), which used a multiplicative aggregation of variable importance values of three models (PLSR, SVMR, and RFR) for identification and selection of spectral bands of importance, led to the selection of 173–271 wavelengths. Model building using the selected wavelengths resulted in further improvements in model fits and prediction accuracy. Serbin et al. (2012), using a different method combined with PLSR, also reported consistently good model prediction and accuracy with fewer wavelengths. This indicated that a large fraction of the wavelengths did not provide predictive power in estimating R_{dark} , which is not surprising given that leaf reflectance spectra are highly collinear, as can be seen from both observations and leaf radiative transfer models such as PROSPECT (Jacquemoud & Baret, 1990). Focusing on specific wavelengths has numerous implications for downstream practise, including in scaling from leaf to vegetation canopy scale and in designing simpler sensors at key wavelengths (Serbin et al., 2012).

4.5 | Prediction of R_{dark} based on O_2 consumption or CO_2 evolution

During leaf respiration, the flux of O_2 consumption relative to CO_2 evolution depends on the substrate being metabolized (1 for carbohydrate and >1 for lipids). Importantly, 20–80% of daily fixed carbon is released back into the atmosphere by whole-plant R_{dark} (Poorter, Remkes, & Lambers, 1990), with leaves accounting for ~50% of whole-plant R_{dark} (Atkin, Scheurwater, & Pons, 2007). It is possible to measure R_{light} or R_{dark} as CO_2 evolution in an open flow through gas exchange system using an infrared gas analyser. Alternatively, if one wishes to measure O_2 consumption, it is necessary to use a closed system to enable a sufficiently large change in O_2 concentration to be detected. The large difference in concentration between CO_2 and O_2 in air generally preclude simultaneous measurements of both without specialised instrumentation (Beckmann, Messinger, Badger,

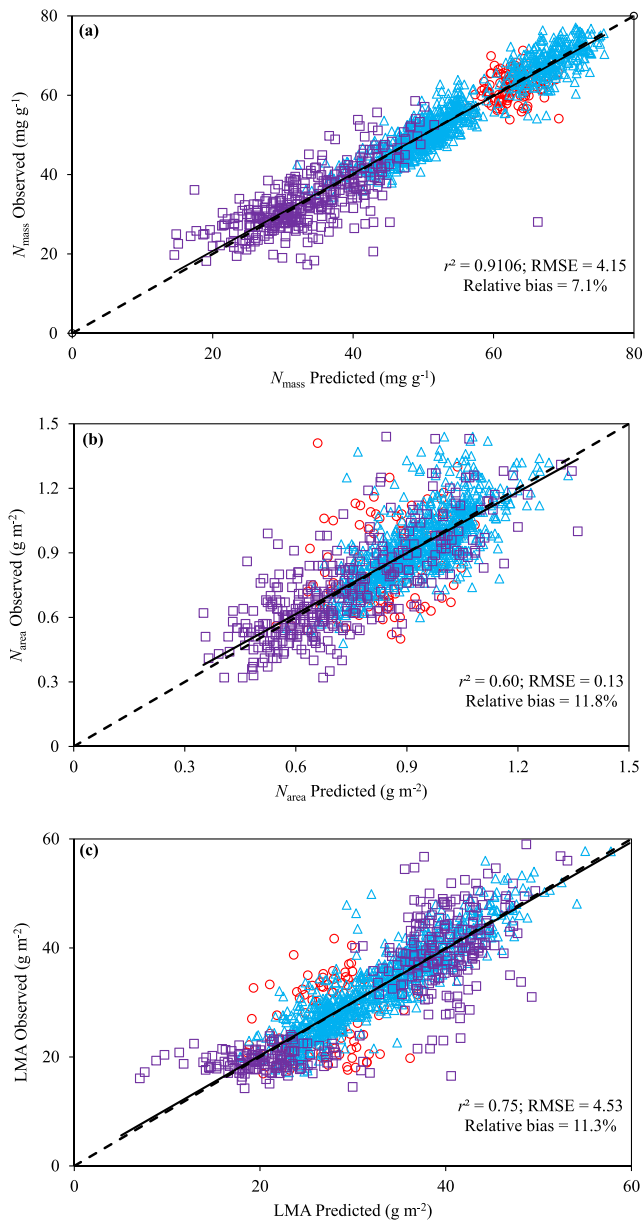


FIGURE 5 Validation of partial least square regression model prediction for nitrogen concentration per unit leaf dry mass (N_{mass} ; a), nitrogen content per unit leaf area (N_{area} ; b), and leaf dry mass per unit area (LMA; c), using 10% of pooled data from Experiment 1 (red circles), Experiment 2 (blue triangles), and Experiment 3 (purple squares) that were not used in developing the model

Wydrzynski, & Hillier, 2009). We chose to measure R_{dark} from O_2 consumption as the rapid measurements allowed more material to be sampled (O'Leary et al., 2017; Scafaro et al., 2017). Although we only validated with data on R_{dark} derived from O_2 consumption, our high-throughput approach can be adapted to measures of R_{dark} derived from CO_2 evolution in cases where sucrose is the predominant respiratory substrate and the respiratory quotient is unity (Lambers et al., 2008).

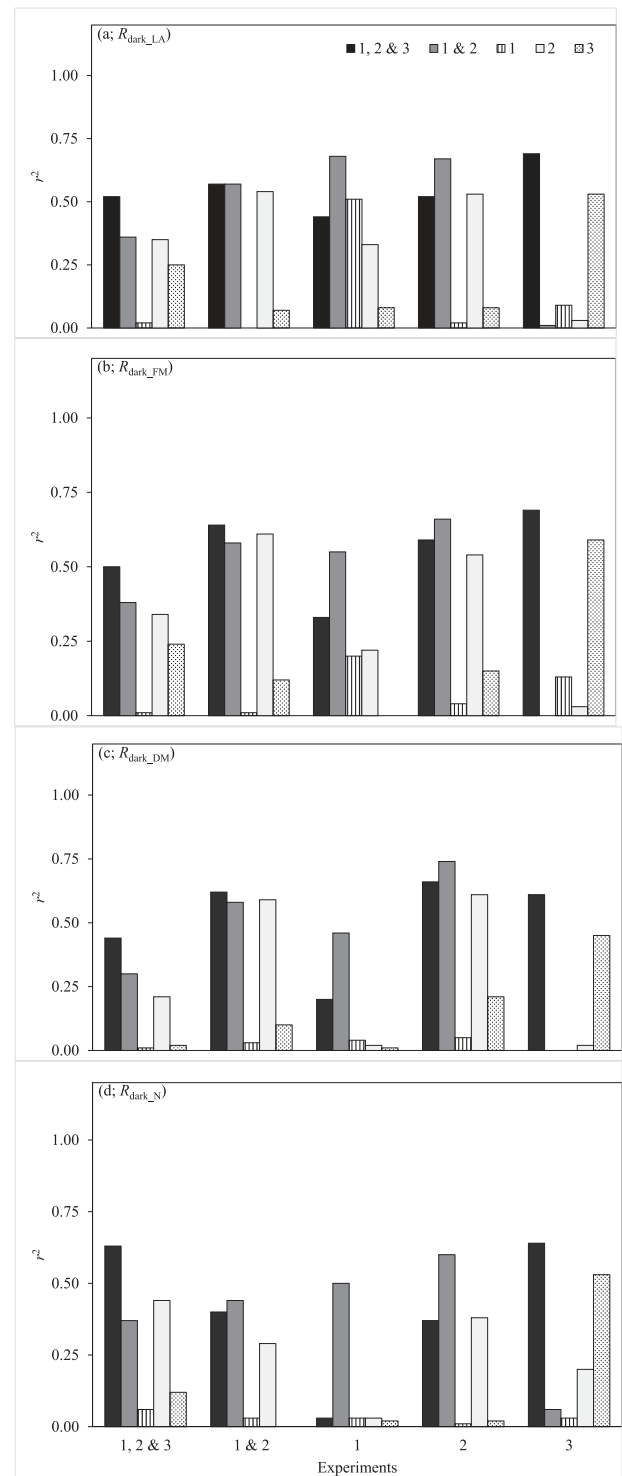


FIGURE 6 Coefficient of determination (r^2) of partial least square regression (PLSR) models used for prediction of leaf dark respiration expressed per square metre of leaf area ($R_{\text{dark_LA}}$; a), per gram of fresh mass ($R_{\text{dark_FM}}$; b), per gram of dry mass ($R_{\text{dark_DM}}$; c), or per gram of leaf nitrogen ($R_{\text{dark_N}}$; d). PLSR models were trained on 90% of data pooled from Experiments 1, 2, and 3 (black bars) or Experiments 1 and 2 (grey bars) or from individual experiments (Experiment 1 [vertical striped bars], Experiment 2 [white bars], or Experiment 3 [dotted bars]) and validated on the test dataset (remaining 10%). See Figure S5 for root mean squared error of PLSR models for predictions of same traits

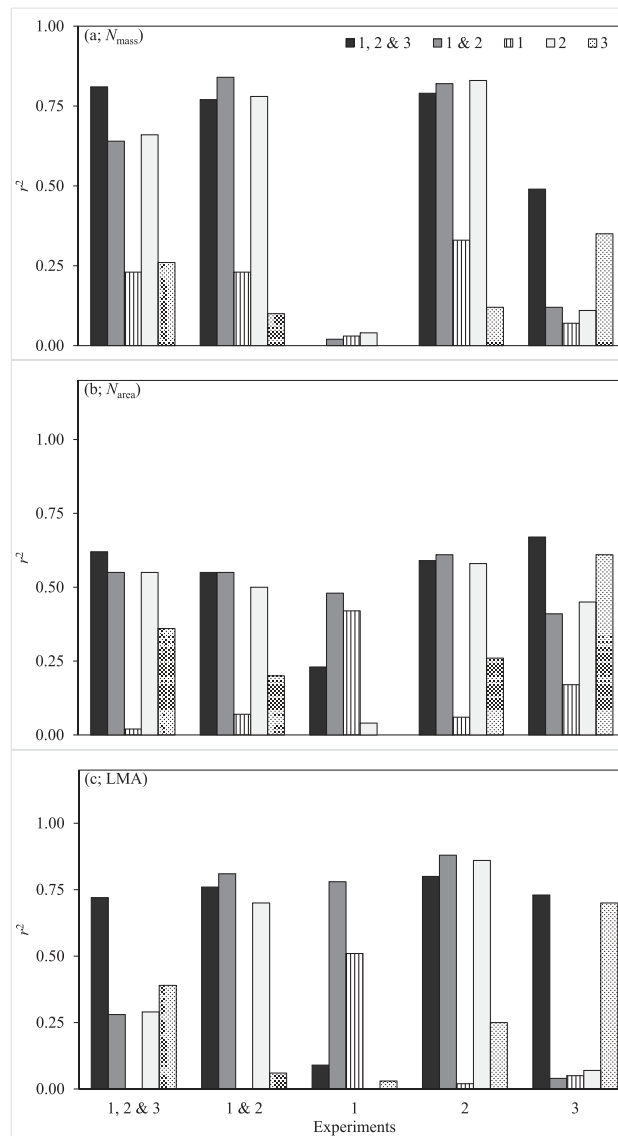


FIGURE 7 Coefficient of determination (r^2) of partial least square regression (PLSR) models used for prediction of leaf nitrogen expressed per gram of DM (N_{mass} ; a) or per square metre of LA (N_{area} ; b), and LMA (c). PLSR models were trained on 90% of data pooled from Experiments 1, 2, and 3 (black bars) or Experiments 1 and 2 (grey bars) or from individual experiments (Experiment 1 [vertical striped bars], Experiment 2 [white bars], or Experiment 3 [dotted bars]) and validated on the test dataset (remaining 10%). See Figure S6 for root mean squared error of PLSR models for predictions of same traits

5 | CONCLUSIONS

Using a diverse set of wheat genotypes measured at different growth stages and grown under varied environmental conditions (light and temperature, either in glasshouses or field settings), we have created a large wheat leaf R_{dark} dataset and found that R_{dark} varied enormously. R_{dark} can be predicted from leaf reflectance spectra, with r^2 as high as 0.63 (when expressed per gram of N with RMSE = 102.4 nmol $\text{O}_2 \text{ g}_N^{-1} \text{ s}^{-1}$ and relative bias = 18.2%). The performance of models built to predict R_{dark} was similar for both PLSR and SVMR approaches. Predictions were not tightly linked to the relationships between leaf R_{dark} and LMA or leaf N. This finding highlights the potential for rapid non-invasive monitoring of various aspects of leaf energy metabolism

in wheat. Such advances will provide opportunities for large scale field experiments to identify variants in wheat R_{dark} , specifically, and wheat energy use efficiency more broadly.

ACKNOWLEDGMENTS

This work was supported by grants from the ARC Centre of Excellence in Plant Energy Biology (CE140100008), the ARC Centre of Excellence for Translational Photosynthesis (CE1401000015), the Australian Government National Collaborative Research Infrastructure Strategy (Australian Plant Phenomics Facility) – PIEPS grant, the International Wheat Yield Partnership and Grains Research Development Council

Grant (ANU00027). We acknowledge the Endeavour Fellowship awarded to S.S. for which part of this research was developed.

CONFLICT OF INTEREST

The authors declare that they have no conflict of interest.

ORCID

Onoriode Coast  <https://orcid.org/0000-0002-5013-4715>

Philippa B. Wilson  <https://orcid.org/0000-0001-9548-691X>

John R. Evans  <https://orcid.org/0000-0003-1379-3532>

A. Harvey Millar  <https://orcid.org/0000-0001-9679-1473>

Owen K. Atkin  <https://orcid.org/0000-0003-1041-5202>

REFERENCES

- Ainsworth, E. A., Serbin, S. P., Skoneczka, J. A., & Townsend, P. A. (2014). Using leaf optical properties to detect ozone effects on foliar biochemistry. *Photosynthesis Research*, 119, 65–76. <https://doi.org/10.1007/s11120-013-9837-y>
- Appaix, F., Minatchy, M. N., Riva-Lavieille, C., Olivares, J., Antonsson, B., & Saks, V. A. (2000). Rapid spectrophotometric method for quantitation of cytochrome c release from isolated mitochondria or permeabilized cells revisited. *Biochimica et Biophysica Acta (BBA)-Bioenergetics*, 1457, 175–181. [https://doi.org/10.1016/S0005-2728\(00\)00098-0](https://doi.org/10.1016/S0005-2728(00)00098-0)
- Armstrong, A. F., Logan, D. C., & Atkin, O. K. (2006). On the developmental dependence of leaf respiration: Responses to short- and long-term changes in growth temperature. *American Journal of Botany*, 93, 1633–1639. <https://doi.org/10.3732/ajb.93.11.1633>
- Armstrong, A. F., Logan, D. C., O'Toole, P., Tobin, A. K., & Atkin, O. K. (2006). Heterogeneity of plant mitochondrial responses underpinning respiratory acclimation to the cold in *Arabidopsis thaliana* leaves. *Plant, Cell & Environment*, 29, 940–949. <https://doi.org/10.1111/j.1365-3040.2005.01475.x>
- Asner, G. P., & Martin, R. E. (2008). Spectral and chemical analysis of tropical forests: Scaling from leaf to canopy levels. *Remote Sensing of Environment*, 112, 3958–3970. <https://doi.org/10.1016/j.rse.2008.07.003>
- Asner, G. P., Martin, R. E., Tupayachi, R., Anderson, C. B., Sinca, F., Carranza-Jiménez, L., & Martínez, P. (2014). Amazonian functional diversity from forest canopy chemical assembly. *Proceedings of the National Academy of Sciences of the United States of America*, 111, 5604–5609. <https://doi.org/10.1073/pnas.1401181111>
- Asner, G. P., Martin, R. E., Tupayachi, R., Emerson, R., Martínez, P., Sinca, F., ... Lugo, A. E. (2011). Taxonomy and remote sensing of leaf mass per area (LMA) in humid tropical forests. *Ecological Applications*, 21, 85–98. <https://doi.org/10.1890/09-1999.1>
- Atkin, O. K., Bloomfield, K. J., Reich, P. B., Tjoelker, M. G., Asner, G. P., Bonal, D., ... Cosio, E. G. (2015). Global variability in leaf respiration in relation to climate, plant functional types and leaf traits. *New Phytologist*, 206, 614–636. <https://doi.org/10.1111/nph.13253>
- Atkin, O. K., Scheurwater, I., & Pons, T. L. (2006). High thermal acclimation potential of both photosynthesis and respiration in two lowland *Plantago* species in contrast to an alpine congeneric. *Global Change Biology*, 12, 500–515. <https://doi.org/10.1111/j.1365-2486.2006.01114.x>
- Atkin, O. K., Scheurwater, I., & Pons, T. L. (2007). Respiration as a percentage of daily photosynthesis in whole plants is homeostatic at moderate, but not high, growth temperatures. *New Phytologist*, 174, 367–380. <https://doi.org/10.1111/j.1469-8137.2007.02011.x>
- Atkin, O. K., & Tjoelker, M. G. (2003). Thermal acclimation and the dynamic response of plant respiration to temperature. *Trends in Plant Science*, 8, 343–351. [https://doi.org/10.1016/S1360-1385\(03\)00136-5](https://doi.org/10.1016/S1360-1385(03)00136-5)
- Barnes, M. L., Breshears, D. D., Law, D. J., van Leeuwen, W. J. D., Monson, R. K., Fojtik, A. C., ... Moore, D. J. P. (2017). Beyond greenness: Detecting temporal changes in photosynthetic capacity with hyperspectral reflectance data. *PLoS ONE*, 12, e0189539. <https://doi.org/10.1371/journal.pone.0189539>
- Beckmann, K., Messinger, J., Badger, M. R., Wydrzynski, T., & Hillier, W. (2009). On-line mass spectrometry: Membrane inlet sampling. *Photosynthesis Research*, 102, 511–522. <https://doi.org/10.1007/s11120-009-9474-7>
- Blackburn, G. A. (2007). Hyperspectral remote sensing of plant pigments. *Journal of Experimental Botany*, 58, 855–867.
- Bolster, K. L., Martin, M. E., & Aber, J. D. (1996). Determination of carbon fraction and nitrogen concentration in tree foliage by near infrared reflectances: A comparison of statistical methods. *Canadian Journal of Forest Research*, 26, 590–600. <https://doi.org/10.1139/x26-068>
- Bouma, T. J., De Visser, R., Van Leeuwen, P. H., De Kock, M. J., & Lambers, H. (1995). The respiratory energy requirements involved in nocturnal carbohydrate export from starch-storing mature source leaves and their contribution to leaf dark respiration. *Journal of Experimental Botany*, 46, 1185–1194. <https://doi.org/10.1093/jxb/46.9.1185>
- Breiman, L. (2001). Random forests. *Machine Learning*, 45, 5–32. <https://doi.org/10.1023/A:1010933404324>
- Byrd, G. T., Sage, R. F., & Brown, R. H. (1992). A comparison of dark respiration between C₃ and C₄ plants. *Plant Physiology*, 100, 191–198. <https://doi.org/10.1104/pp.100.1.191>
- Cassman, K. G. (1999). Ecological intensification of cereal production systems: Yield potential, soil quality, and precision agriculture. *Proceedings of the National Academy of Sciences of the United States of America*, 96, 5952–5959. <https://doi.org/10.1073/pnas.96.11.5952>
- R Core Team (2018). R: A language and environment for statistical computing. R Foundation for statistical computing, Vienna, Austria. URL <https://www.R-project.org/>.
- Curran, P. J. (1989). Remote sensing of foliar chemistry. *Remote Sensing of Environment*, 30, 271–278. [https://doi.org/10.1016/0034-4257\(89\)90069-2](https://doi.org/10.1016/0034-4257(89)90069-2)
- Dechant, B., Cuntz, M., Vohland, M., Schulz, E., & Doktor, D. (2017). Estimation of photosynthesis traits from leaf reflectance spectra: Correlation to nitrogen content as the dominant mechanism. *Remote Sensing of Environment*, 196, 279–292. <https://doi.org/10.1016/j.rse.2017.05.019>
- Doughty, C. E., Asner, G. P., & Martin, R. E. (2011). Predicting tropical plant physiology from leaf and canopy spectroscopy. *Oecologia*, 165, 289–299. <https://doi.org/10.1007/s00442-010-1800-4>
- Ecarnot, M., Compan, F., & Roumet, P. (2013). Assessing leaf nitrogen content and leaf mass per unit area of wheat in the field throughout plant cycle with a portable spectrometer. *Field Crops Research*, 140, 44–50. <https://doi.org/10.1016/j.fcr.2012.10.013>
- Evans, J. R. (1989a). Photosynthesis and nitrogen relationships in leaves of C₃ plants. *Oecologia*, 78, 9–19. <https://doi.org/10.1007/BF00377192>
- Evans, J. R. (1989b). Partitioning of nitrogen between and within leaves grown under different irradiances. *Functional Plant Biology*, 16, 533–548. <https://doi.org/10.1071/PP9890533>
- Evans, J. R., & Terashima, I. (1988). Photosynthetic characteristics of spinach leaves grown with different nitrogen treatments. *Plant and Cell Physiology*, 29, 157–165. <https://doi.org/10.1093/oxfordjournals.pcp.a077462>

- Fan, R., Sun, J., Yang, F., Li, M., Zheng, Y., Zhong, Q., & Cheng, D. (2017). Divergent scaling of respiration rates to nitrogen and phosphorus across four woody seedlings between different growing seasons. *Ecology and Evolution*, 7, 8761–8769. <https://doi.org/10.1002/ece3.3419>
- Feilhauer, H., Asner, G. P., & Martin, R. E. (2015). Multi-method ensemble selection of spectral bands related to leaf biochemistry. *Remote Sensing of Environment*, 164, 57–65. <https://doi.org/10.1016/j.rse.2015.03.033>
- Field, C., & Mooney, H. A. (1986). The photosynthesis-nitrogen relationship in wild plants. In T. J. Givnish (Ed.), *On the economy of form and function* (pp. 25–55). Cambridge: Cambridge University Press.
- Furbank, R. T., von Caemmerer, S., Sheehy, J., & Edwards, G. (2009). C₄ rice: A challenge for plant phenomics. *Functional Plant Biology*, 36, 845–856. <https://doi.org/10.1071/FP09185>
- Godfray, H. C. J., Beddington, J. R., Crute, I. R., Haddad, L., Lawrence, D., Muir, J. F., ... Toulmin, C. (2010). Food security: The challenge of feeding 9 billion people. *Science*, 327, 812–818. <https://doi.org/10.1126/science.1185383>
- Goldsmith, P. D., Gunjal, K., & Ndarishikanye, B. (2004). Rural–urban migration and agricultural productivity: The case of Senegal. *Agricultural Economics*, 31, 33–45. <https://doi.org/10.1016/j.agecon.2003.01.002>
- Guerrero, C., Stenberg, B., Wetterlind, J., Viscarra Rossel, R. A., Maestre, F. T., Mouazen, A. M., ... Kuang, B. (2014). Assessment of soil organic carbon at local scale with spiked NIR calibrations: Effects of selection and extra-weighting on the spiking subset. Spiking and extra-weighting to improve soil organic carbon predictions with NIR. *European Journal of Soil Science*, 65, 248–263. <https://doi.org/10.1111/ejss.12129>
- Guerrero, C., Wetterlind, J., Stenberg, B., Mouazen, A. M., Gabarrón-Galeote, M. A., Ruiz-Sinoga, J. D., ... Viscarra Rossel, R. A. (2016). Do we really need large spectral libraries for local scale SOC assessment with NIR spectroscopy? *Soil and Tillage Research*, 155, 501–509. <https://doi.org/10.1016/j.still.2015.07.008>
- Guerrero, C., Zornoza, R., Gómez, I., & Mataix-Beneyto, J. (2010). Spiking of NIR regional models using samples from target sites: Effect of model size on prediction accuracy. *Geoderma*, 158, 66–77. <https://doi.org/10.1016/j.geoderma.2009.12.021>
- Gutierrez, M., Reynolds, M. P., & Klatt, A. R. (2010). Association of water spectral indices with plant and soil water relations in contrasting wheat genotypes. *Journal of Experimental Botany*, 61, 3291–3303. <https://doi.org/10.1093/jxb/erq156>
- Hachiya, T., Terashima, I., & Noguchi, K. (2007). Increase in respiratory cost at high growth temperature is attributed to high protein turnover cost in *Petunia* × *hybrida* petals. *Plant, Cell & Environment*, 30, 1269–1283. <https://doi.org/10.1111/j.1365-3040.2007.01701.x>
- Harrison, M. T., Edwards, E. J., Farquhar, G. D., Nicotra, A. B., & Evans, J. R. (2009). Nitrogen in cell walls of sclerophyllous leaves accounts for little of the variation in photosynthetic nitrogen-use efficiency. *Plant, Cell & Environment*, 32, 259–270. <https://doi.org/10.1111/j.1365-3040.2008.01918.x>
- Hauben, M., Haesendonckx, B., Standaert, E., Van Der Kelen, K., Azmi, A., Akpo, H., ... Lambert, B. (2009). Energy use efficiency is characterized by an epigenetic component that can be directed through artificial selection to increase yield. *Proceedings of the National Academy of Sciences of the United States of America*, 106, 20109–20114. <https://doi.org/10.1073/pnas.0908755106>
- Heckmann, D., Schlüter, U., & Weber, A. P. (2017). Machine learning techniques for predicting crop photosynthetic capacity from leaf reflectance spectra. *Molecular Plant*, 10, 878–890. <https://doi.org/10.1016/j.molp.2017.04.009>
- Hirose, T., & Werger, M. J. (1987). Nitrogen use efficiency in instantaneous and daily photosynthesis of leaves in the canopy of a *Solidago altissima* stand. *Physiologia Plantarum*, 70, 215–222. <https://doi.org/10.1111/j.1399-3054.1987.tb06134.x>
- Hoefnagel, M. H. N., & Wiskich, J. T. (1998). Activation of the plant alternative oxidase by high reduction levels of the Q-pool and pyruvate. *Archives of Biochemistry and Biophysics*, 355, 262–270. <https://doi.org/10.1006/abbi.1998.0737>
- Hsu, C. W., Chang, C. C., & Lin C. J. (2003). A practical guide to support vector classification. Technical Report, Department of Computer Science, National Taiwan University, Taipei, Taiwan. pp 1–16. Retrieved from <http://www.csie.ntu.edu.tw/~cjlin/papers/guide/guide.pdf>.
- Hu, Z., Vanderhaeghen, R., Cools, T., Wang, Y., De Clercq, I., Leroux, O., ... Hilson, P. (2016). Mitochondrial defects confer tolerance against cellulose deficiency. *The Plant Cell*, 28, 2276–2290. <https://doi.org/10.1105/tpc.16.00540>
- Hurry, V., Igamberdiev, A. U., Keerberg, O., Parnik, T. R., Atkin, O. K., Zaragoza-Castells, J., ... Ribas-Carbó, M. (2005). Respiration in photosynthetic cells: Gas exchange components, interactions with photorespiration and the operation of mitochondria in the light. In H. Lambers, & M. Ribas-Carbó (Eds.), *Plant respiration: From cell to ecosystem* (Vol. 18) (pp. 43–61). Dordrecht, The Netherlands: Springer. https://doi.org/10.1007/1-4020-3589-6_4
- Intergovernmental Panel on Climate Change (2013). Summary for policymakers. In T. F. Stocker, D. Qin, G. K. Plattner, et al. (Eds.), *Climate change 2013: The physical science basis. Contribution of working group I to the Fifth Assessment Report of the Intergovernmental Panel on Climate Change* (pp. 3–29). Cambridge: Cambridge University Press.
- Ishell, R. F. (2002). *The Australian soil classification*. Collingwood: CSIRO Publishing. <https://doi.org/10.1071/9780643069817>
- Jacquemoud, S., & Baret, F. (1990). PROSPECT: A model of leaf optical properties spectra. *Remote Sensing of Environment*, 34, 75–91. [https://doi.org/10.1016/0034-4257\(90\)90100-Z](https://doi.org/10.1016/0034-4257(90)90100-Z)
- Jacquemoud, S., Ustin, S. L., Verdebout, J., Schmuck, G., Andreoli, G., & Hosgood, B. (1996). Estimating leaf biochemistry using the PROSPECT leaf optical properties model. *Remote Sensing of Environment*, 56, 194–202. [https://doi.org/10.1016/0034-4257\(95\)00238-3](https://doi.org/10.1016/0034-4257(95)00238-3)
- Jullien, A., Allirand, J. M., Mathieu, A., Andrieu, B., & Ney, B. (2009). Variations in leaf mass per area according to N nutrition, plant age, and leaf position reflect ontogenetic plasticity in winter oilseed rape (*Brassica napus* L.). *Field Crops Research*, 114, 188–197. <https://doi.org/10.1016/j.fcr.2009.07.015>
- Kok, B. (1948). A critical consideration of the quantum yield of *Chlorella*-photosynthesis. *Enzymologia*, 13, 1–56.
- Laisk, A. K. (1977). *Kinetics of photosynthesis and photorespiration in C₃-plants*. Moscow: Nauka.
- Lambers, H., Chapin, F. S., & Pons, T. L. (2008). *Plant physiological ecology*. USA: Springer. <https://doi.org/10.1007/978-0-387-78341-3>
- Loomis, R. S., & Williams, W. A. (1969). Productivity and the morphology of crop stands. In J. D. Eastin, F. A. Haskin, C. Y. Sullivan, & C. H. M. Van Bavel (Eds.), *Physiological aspects of crop yield* (pp. 27–47). Winconsin: American Society of Agronomy.
- Loreto, F., Velikova, V., & Di Marco, G. (2001). Respiration in the light measured by CO₂-¹²C emission in CO₂-¹³C atmosphere in maize leaves. *Australian Journal of Plant Physiology*, 28, 1103–1108. <https://doi.org/10.1071/PP01091>
- Lusk, C. H., Reich, P. B., Montgomery, R. A., Ackerly, D. D., & Cavender-Bares, J. (2008). Why are evergreen leaves so contrary about shade? *Trends in Ecology & Evolution*, 23, 299–303. <https://doi.org/10.1016/j.tree.2008.02.006>
- Makino, Y., Ichimura, M., Kawagoe, Y., & Oshita, S. (2007). Cytochrome c oxidase as a cause of variation in oxygen uptake rates among

- vegetables. *Journal of the American Society for Horticultural Science*, 132, 239–245. <https://doi.org/10.21273/JASHS.132.2.239>
- Makino, Y., Ichimura, M., Oshita, S., Kawagoe, Y., & Yamanaka, H. (2010). Estimation of oxygen uptake rate of tomato (*Lycopersicon esculentum* Mill.) fruits by artificial neural networks modelled using near-infrared spectral absorbance and fruit mass. *Food Chemistry*, 121, 533–539. <https://doi.org/10.1016/j.foodchem.2009.12.043>
- Martin, A. R., Hale, C. E., Cerabolini, B. E., Cornelissen, J. H., Craine, J., Gough, W. A., ... , Tirona, C. K. (2018). Inter- and intraspecific variation in leaf economic traits in wheat and maize. *AoB Plants*, 10, p.ply006. <https://doi.org/10.1093/aobpla/ply006>
- Martin, M. E., & Aber, J. D. (1997). High spectral resolution remote sensing of forest canopy lignin, nitrogen, and ecosystem processes. *Ecological Applications*, 7, 431–443. [https://doi.org/10.1890/1051-0761\(1997\)007\[0431:HSRRO\]2.0.CO;2](https://doi.org/10.1890/1051-0761(1997)007[0431:HSRRO]2.0.CO;2)
- Mason, M. G., Nicholls, P., & Cooper, C. E. (2014). Re-evaluation of the near infrared spectra of mitochondrial cytochrome *c* oxidase: Implications for non invasive *in vivo* monitoring of tissues. *Biochimica et Biophysica Acta (BBA)-Bioenergetics*, 1837, 882–1891. <https://doi.org/10.1016/j.bbabo.2014.08.005>
- Mevik, B.-H., Wehrens, R., Liland, K. H. (2016). PLS: Partial least squares and principal component regression. R package version 2.6–0. <https://CRAN.R-project.org/package=pls>
- Meyer, D., Dimitriadou, E., Hornik, K., Weingessel, A., & Leisch, F. (2017). e1071: Misc functions of the Department of Statistics, probability theory group (Formerly: E1071), TU Wien. R package version 1.6–8. <https://CRAN.R-project.org/package=e1071>
- Millar, A. H., Whelan, J., Soole, K. L., & Day, D. A. (2011). Organization and regulation of mitochondrial respiration in plants. *Annual Review of Plant Biology*, 62, 79–104. <https://doi.org/10.1146/annurev-arplant-042110-103857>
- Miroslavov, E. A., & Kravkina, I. M. (1991). Comparative analysis of chloroplasts and mitochondria in leaf chlorenchyma from mountain plants grown at different altitudes. *Annals of Botany*, 68, 195–200. <https://doi.org/10.1093/oxfordjournals.aob.a088244>
- Montesinos-López, A., Montesinos-López, O. A., Cuevas, J., Mata-López, W. A., Burgueño, J., Mondal, S., ... Crossa, J. (2017). Genomic Bayesian functional regression models with interactions for predicting wheat grain yield using hyper-spectral image data. *Plant Methods*, 13, 62. <https://doi.org/10.1186/s13007-017-0212-4>
- Montesinos-López, O. A., Montesinos-López, A., Crossa, J., los Campos, G., Alvarado, G., Suchismita, M., ... Burgueño, J. (2017). Predicting grain yield using canopy hyperspectral reflectance in wheat breeding data. *Plant Methods*, 13, 4. <https://doi.org/10.1186/s13007-016-0154-2>
- Mooney, H. A. (1963). Physiological ecology of coastal, subalpine, and alpine populations of *Polygonum bistortoides*. *Ecology*, 44, 812–816. <https://doi.org/10.2307/1933039>
- Noguchi, K. (2005). Effects of light intensity and carbohydrate status on leaf and root respiration. In H. Lambers, & M. Ribas-Carbo (Eds.), *Plant respiration from cell to ecosystem* (pp. 63–83). Dordrecht: Springer.
- Noguchi, K., & Yoshida, K. (2008). Interaction between photosynthesis and respiration in illuminated leaves. *Mitochondrion*, 8, 87–99. <https://doi.org/10.1016/j.mito.2007.09.003>
- O'Leary, B. M., Lee, C. P., Atkin, O. K., Cheng, R., Brown, T. B., & Millar, A. H. (2017). Variation in leaf respiration rates at night correlates with carbohydrate and amino acid supply. *Plant Physiology*, 174, 2261–2273. <https://doi.org/10.1104/pp.17.00610>
- Oleksyn, J., Modrzyński, J., Tjoelker, M. G., Zytkowski, R., Reich, P. B., & Karolewski, P. (1998). Growth and physiology of *Picea abies* populations from elevational transects: Common garden evidence for altitudinal ecotypes and cold adaptation. *Functional Ecology*, 12, 573–590. <https://doi.org/10.1046/j.1365-2435.1998.00236.x>
- Pärnik, T., & Keerberg, O. (1995). Decarboxylation of primary and end products of photosynthesis at different oxygen concentrations. *Journal of Experimental Botany*, 46, 1439–1447. https://doi.org/10.1093/jxb/46.special_issue.1439
- Parry, M. A. J., Madgwick, P. J., Carvalho, J. F. C., & Andralojc, P. J. (2007). Prospects for increasing photosynthesis by overcoming the limitations of Rubisco. *The Journal of Agricultural Science*, 145, 31. <https://doi.org/10.1017/S0021859606006666>
- Peraudeau, S., Lafarge, T., Roques, S., Quiñones, C. O., Clement-Vidal, A., Ouwerkerk, P. B., ... Dingkuhn, M. (2015). Effect of carbohydrates and night temperature on night respiration in rice. *Journal of Experimental Botany*, 66, 3931–3944. <https://doi.org/10.1093/jxb/erv193>
- Poorter, H., Niinemets, U., Poorter, L., Wright, I. J., & Villar, R. (2009). Causes and consequences of variation in leaf mass per area (LMA): A meta-analysis. *New Phytologist*, 183, 565–588. <https://doi.org/10.1111/j.1469-8137.2009.02830.x>
- Poorter, H., Remkes, C., & Lambers, H. (1990). Carbon and nitrogen economy of 24 wild species differing in relative growth rate. *Plant Physiology*, 94, 621–627. <https://doi.org/10.1104/pp.94.2.621>
- Ramirez, J. A., Posada, J. M., Handa, I. T., Hoch, G., Vohland, M., Messier, C., & Reu, B. (2015). Near-infrared spectroscopy (NIRS) predicts non-structural carbohydrate concentrations in different tissue types of a broad range of tree species. *Methods in Ecology and Evolution*, 6, 1018–1025. <https://doi.org/10.1111/2041-210X.12391>
- Reich, P. B., Tjoelker, M. G., Pregitzer, K. S., Wright, I. J., Oleksyn, J., & Machado, J. L. (2008). Scaling of respiration to nitrogen in leaves, stems and roots of higher land plants. *Ecology Letters*, 11, 793–801. <https://doi.org/10.1111/j.1461-0248.2008.01185.x>
- Reich, P. B., & Walters, M. B. (1994). Photosynthesis-nitrogen relations in Amazonian tree species. II. Variation in nitrogen vis-a-vis specific leaf area influences mass- and area-based expressions. *Oecologia*, 97, 73–81. <https://doi.org/10.1007/BF00317910>
- Reich, P. B., Walters, M. B., & Ellsworth, D. S. (1997). From tropics to tundra: Global convergence in plant functioning. *Proceedings of the National Academy of Sciences of the United States of America*, 94, 13730–13734. <https://doi.org/10.1073/pnas.94.25.13730>
- Reich, P. B., Walters, M. B., Ellsworth, D. S., Vose, J. M., Volin, J. C., Gresham, C., & Bowman, W. D. (1998). Relationships of leaf dark respiration to leaf nitrogen, specific leaf area and leaf life-span: A test across biomes and functional groups. *Oecologia*, 114, 471–482. <https://doi.org/10.1007/s004420050471>
- Reich, P. B., Walters, M. B., Tjoelker, M., Vanderklein, D., & Buschena, C. (1998). Photosynthesis and respiration rates depend on leaf and root morphology and nitrogen concentration in nine boreal tree species differing in relative growth rate. *Functional Ecology*, 12, 395–405. <https://doi.org/10.1046/j.1365-2435.1998.00209.x>
- Ryan, M. G. (1991). Effects of climate change on plant respiration. *Ecological Applications*, 1, 157–167. <https://doi.org/10.2307/1941808>
- Scafaro, A. P., Negrini, A. C. A., O'Leary, B., Rashid, F. A. A., Hayes, L., Fan, Y., ... Atkin, O. K. (2017). The combination of gas-phase fluorophore technology and automation to enable high-throughput analysis of plant respiration. *Plant Methods*, 13, 16. <https://doi.org/10.1186/s13007-017-0169-3>
- Serbin, S. P., Dillaway, D. N., Kruger, E. L., & Townsend, P. A. (2012). Leaf optical properties reflect variation in photosynthetic metabolism and its sensitivity to temperature. *Journal of Experimental Botany*, 63, 489–502. <https://doi.org/10.1093/jxb/err294>
- Sew, Y. S., Ströher, E., Holzmann, C., Huang, S., Taylor, N. L., Jordana, X., & Millar, A. H. (2013). Multiplex micro-respiratory measurements of

- Arabidopsis tissues. *New Phytologist*, 200, 922–932. <https://doi.org/10.1111/nph.12394>
- Silva-Pérez, V., Molero, G., Serbin, S. P., Condon, A. G., Reynolds, M. P., Furbank, R. T., & Evans, J. R. (2018). Hyperspectral reflectance as a tool to measure biochemical and physiological traits in wheat. *Journal of Experimental Botany*, 69, 483–496. <https://doi.org/10.1093/jxb/erx421>
- Sims, D. A., & Gamon, J. A. (2003). Estimation of vegetation water content and photosynthetic tissue area from spectral reflectance: A comparison of indices based on liquid water and chlorophyll absorption features. *Remote Sensing of Environment*, 84, 526–537. [https://doi.org/10.1016/S0034-4257\(02\)00151-7](https://doi.org/10.1016/S0034-4257(02)00151-7)
- Thissen, U., Pepers, M., Üstün, B., Melssen, W. J., & Buydens, L. M. C. (2004). Comparing support vector machines to PLS for spectral regression applications. *Chemometrics and Intelligent Laboratory Systems*, 73, 169–179. <https://doi.org/10.1016/j.chemolab.2004.01.002>
- Tilman, D., Balzer, C., Hill, J., & Befort, B. L. (2011). Global food demand and the sustainable intensification of agriculture. *Proceedings of the National Academy of Sciences of the United States of America*, 108, 20260–20264. <https://doi.org/10.1073/pnas.1116437108>
- Tilman, D., Cassman, K. G., Matson, P. A., Naylor, R., & Polasky, S. (2002). Agricultural sustainability and intensive production practices. *Nature*, 418, 671–677. <https://doi.org/10.1038/nature01014>
- Umbach, A. L., Lacey, E. P., & Richter, S. J. (2009). Temperature-sensitive alternative oxidase protein content and its relationship to floral reflectance in natural *Plantago lanceolata* populations. *New Phytologist*, 181, 662–671. <https://doi.org/10.1111/j.1469-8137.2008.02683.x>
- United Nations Department of Economic and Social Affairs Population Division (2015) World population prospects: The 2015 revision, methodology of the United Nations population estimates and projections. Working Paper No. ESA/P/WP.242. United Nations, New York.
- Vanlerberghe, G. C., & McIntosh, L. (1997). Alternative oxidase: From gene to function. *Annual Review of Plant Biology*, 48, 703–734. <https://doi.org/10.1146/annurev.arplant.48.1.703>
- Vapnik, V. N. (1995). *The nature of statistical learning theory*. New York: Springer-Verlag Inc. <https://doi.org/10.1007/978-1-4757-2440-0>
- Weber, V. S., Araus, J. L., Cairns, J. E., Sanchez, C., Melchinger, A. E., & Orsini, E. (2012). Prediction of grain yield using reflectance spectra of canopy and leaves in maize plants grown under different water regimes. *Field Crops Research*, 128, 82–90. <https://doi.org/10.1016/j.fcr.2011.12.016>
- Wilson, D., & Jones, J. G. (1982). Effect of selection for dark respiration rate of mature leaves on crop yields of *Lolium perenne* cv. S23. *Annals of Botany*, 49, 313–320. <https://doi.org/10.1093/oxfordjournals.aob.a086255>
- Wold, S., Sjöström, M., & Eriksson, L. (2001). PLS-regression: A basic tool of chemometrics. *Chemometrics and Intelligent Laboratory Systems*, 58, 109–130. [https://doi.org/10.1016/S0169-7439\(01\)00155-1](https://doi.org/10.1016/S0169-7439(01)00155-1)
- Wright, I. J., Reich, P. B., Atkin, O. K., Lusk, C. H., Tjoelker, M. G., & Westoby, M. (2006). Irradiance, temperature and rainfall influence leaf dark respiration in woody plants: Evidence from comparisons across 20 sites. *New Phytologist*, 169, 309–319. <https://doi.org/10.1111/j.1469-8137.2005.01590.x>
- Wright, I. J., Reich, P. B., Westoby, M., Ackerly, D. D., Baruch, Z., Bongers, F., ... Villar, R. (2004). The worldwide leaf economics spectrum. *Nature*, 428, 821–827. <https://doi.org/10.1038/nature02403>
- Xiang, S., Reich, P. B., Sun, S., & Atkin, O. K. (2013). Contrasting leaf trait scaling relationships in tropical and temperate wet forest species. *Functional Ecology*, 27, 522–534. <https://doi.org/10.1111/1365-2435.12047>
- Xiao, Z., & Ximing, C. (2011). Climate change impacts on global agricultural land availability. *Environmental Research Letters*, 6, 014014. <https://doi.org/10.1088/1748-9326/6/1/014014>
- Yendrek, C. R., Tomaz, T., Montes, C. M., Cao, Y., Morse, A. M., Brown, P. J., ... Ainsworth, E. A. (2017). High-throughput phenotyping of maize leaf physiological and biochemical traits using hyperspectral reflectance. *Plant Physiology*, 173, 614–626. <https://doi.org/10.1104/pp.16.01447>
- Zadoks, J. C., Chang, T. T., & Konzak, C. F. (1974). A decimal code for the growth stages of cereals. *Weed Research*, 14, 415–421. <https://doi.org/10.1111/j.1365-3180.1974.tb01084.x>

SUPPORTING INFORMATION

Additional supporting information may be found online in the Supporting Information section at the end of the article.

Table S1. Genotypes used for study.

Table S2. Foliar traits of wheat genotypes for Experiment 1 under different growth irradiance and temperature conditions averaged for three cultivars.

Table S3. Means, mean squares and F probabilities of ANOVAs for foliar traits examined during Experiment 2 for different genotypes and at different growth stages (GS).

Table S4. Means, mean squares and F probabilities of ANOVAs for foliar traits examined during Experiment 3 for different genotypes and at different growth stages (GS).

Table S5. Squared Pearson correlation (r^2) for predictions of leaf dark respiration (R_{dark} , expressed per metre of leaf area (LA), per gram of fresh mass (FM) and dry mass (DM), and leaf nitrogen), nitrogen (expressed per gram of DM and per metre of LA), and leaf mass per unit area (LMA), across all experiments, by the three models using either the continuous, full-spectrum data (350–2500 nm) or a spectral subset selected based on coefficient weightings of a multi-method ensemble developed by Feilhauer et al. (2015).

Table S6. Summary of different trait-based and reflectance-based regression models for leaf dark respiration expressed per square metre of leaf area ($R_{\text{dark_LA}}$). Model predictors are either reflectance, or measured leaf traits – leaf nitrogen (expressed per gram of DM, N_{mass} ; and per metre of LA, N_{area}), and leaf mass per unit area (LMA). The coefficient of determination, r^2 , is shown for all models.

Figure S1 Display showing green mesh suspended by metal cages used to achieve low light (photosynthetic photon flux density of 150–200 $\mu\text{mol m}^{-2} \text{s}^{-1}$ i.e. 25% of ambient) intensity during Experiment 1.

Figure S2. Mean (\pm standard deviation), minimum and maximum leaf reflectance (top panels) of wheat (a–c) and spectral coefficients of variation (d–e) for Experiment 1 (left panels), Experiment 2 (middle panels) and Experiment 3 (right panels).

Figure S3. Relationships between $R_{\text{dark_LA}}$ and (a–c) leaf nitrogen per square metre of leaf area (N_{area}), (d–f) leaf mass per area (LMA), and (g–i) between $R_{\text{dark_DM}}$ and leaf nitrogen per gram of leaf dry mass (N_{mass}) for Experiment 1 (left panels), Experiment 2 (middle panels) and Experiment 3 (right panels). Pearson correlation coefficients (r) for data pooled from Experiments 1, 2 and 3 were 0.16, 0.27 and

0.38, respectively for $R_{\text{dark_LA}}$ vs N_{area} , $R_{\text{dark_LA}}$ vs LMA, and $R_{\text{dark_DM}}$ vs N_{mass} .

Figure S4. Relationship between leaf nitrogen (per square metre of leaf area, N_{area}) and leaf mass per area (LMA) for Experiment 1 (a), Experiment 2 (b) and Experiment 3 (c). For the pooled data Pearson correlation coefficients (r) was 0.12 ($P < 0.001$).

Figure S5. Root mean squared error (RMSE) of PLSR model used for prediction of leaf dark respiration per square metre of leaf area ($R_{\text{dark_LA}}$; a), per gram of fresh mass ($R_{\text{dark_FM}}$; b), per gram of dry mass ($R_{\text{dark_DM}}$; c), or per gram of leaf nitrogen ($R_{\text{dark_N}}$; d). PLSR models were trained on 90% of data pooled from Experiments 1, 2 and 3 (black bars) or Experiments 1 and 2 (grey bars) or from individual experiments (Experiment 1 (vertical striped bars), Experiment 2 (white bars), or Experiment 3 (dotted bars)) and validated on the test dataset (remaining 10%).

Figure S6. Root mean squared error (RMSE) of PLSR model used for prediction of leaf nitrogen per gram of DM (N_{mass} ; a) or per square metre of LA (N_{area} ; b), and LMA (c). PLSR models were trained on 90% of data pooled from Experiments 1, 2 and 3 (black bars) or Experiments 1 and 2 (grey bars) or from individual experiments (Experiment 1 (vertical striped bars), Experiment 2 (white bars), or Experiment 3 (dotted bars)) and validated on the test dataset (remaining 10%).

Text S1. Multi-method ensemble

How to cite this article: Coast O, Shah S, Ivakov A, et al. Predicting dark respiration rates of wheat leaves from hyperspectral reflectance. *Plant Cell Environ.* 2019;42: 2133–2150. <https://doi.org/10.1111/pce.13544>